BigDIA
BIG DATA AND INFORMATION ANALYTICS

The 9th International Conference on Big Data and Information Analytics (BigDIA 2023)

海南大学 HAINAN UNIVERSITY

Design Automation of Intelligent Robots: Key Technologies and Applications

Zhun Fan

Shantou University

2023.12.17

Background

汕頭大學 SHANTOU UNIVERSITY

Current Status of Domestic Industrial Development

The escalating 'chip war' between the US and China, leading to increased sanctions on China's IC industry, highlights the urgent need for us to develop our own design tools for the semiconductor sector.


Bureau of Industry and Security
U.S. Department of Commerce

FOR IMMEDIATE RELEASE
August 12, 2022
https://bis.doc.gov

BUREAU OF INDUSTRY AND SECURITY
Office of Congressional and Public Affairs
Media Contact: OCPA@bis.doc.gov

Commerce Implements New Multilateral Controls on Advanced Semiconductor and Gas Turbine Engine Technologies

WASHINGTON, D.C. – Today, the Commerce Department's Bureau of Industry and Security (BIS) issued an interim final rule that establishes new export controls on four technologies that meet the criteria for emerging and foundational technologies under Section 1758 of the Export Control Reform Act (ECRA) and are essential to the national security of the United States. These Section 1758 technologies support the production of advanced semiconductors and gas turbine engines. These four technologies are among the items that the 42 Participating States of the Wassenaar Arrangement reached consensus to control at the December 2021 Plenary. The United States additionally controls a wider range of technologies, including additional equipment, software, and technology used to produce semiconductors, beyond the items agreed upon in the Wassenaar Arrangement.

The U.S. Department of Commerce has implemented new export controls on EDA tools.

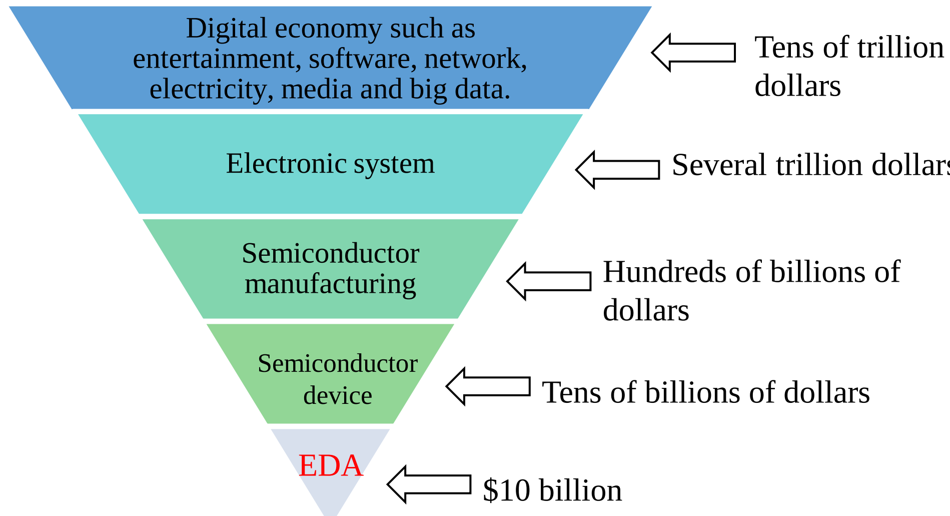

EDA (Electronic Design Automation) is an indispensable and crucial component in chip IC design, serving as the cornerstone of the entire chip industry chain and often referred to as the "mother of chips".

- The '14th Five-Year Plan' of China explicitly ranks integrated circuits as the third key area among the seven frontiers of scientific and technological development. Among these, design tools take precedence within the field of integrated circuits.

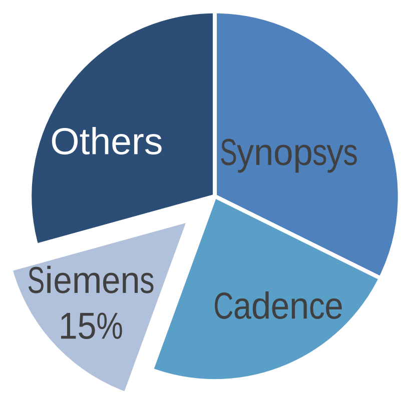

EDA Tools Market Share & Size

Background

Current Status of Domestic Robotic Industry

In China, most robots are primarily designed using reverse engineering, meaning that the original designs are borrowed from foreign brands. The capability and level of forward design are the bottlenecks restricting the original design of China's own robotic brands.

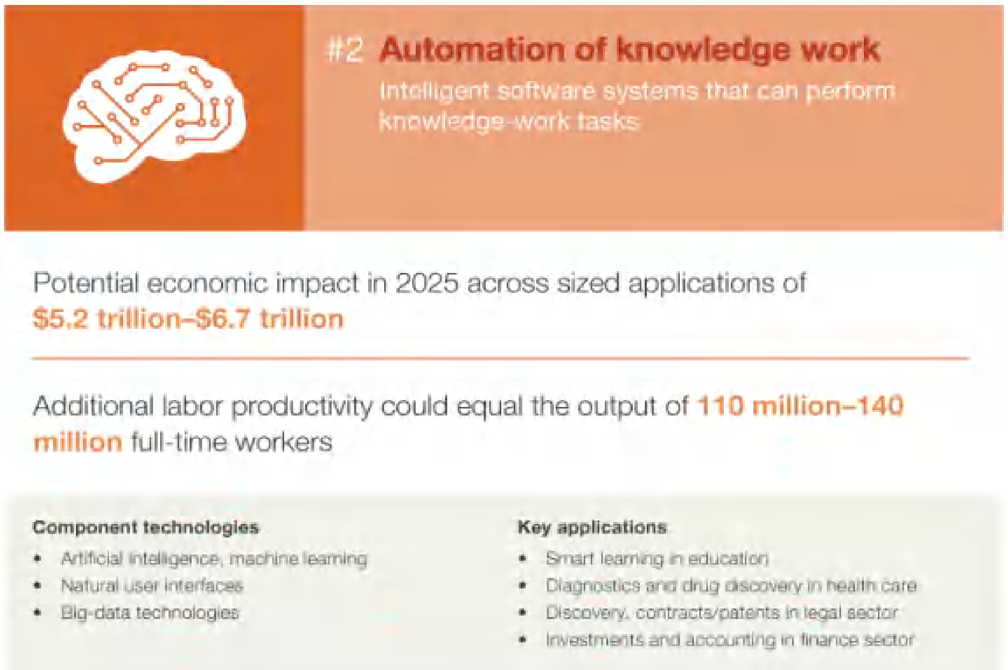

According to a McKinsey report, automation of knowledge work is considered the second most disruptive technology of the 21st century.

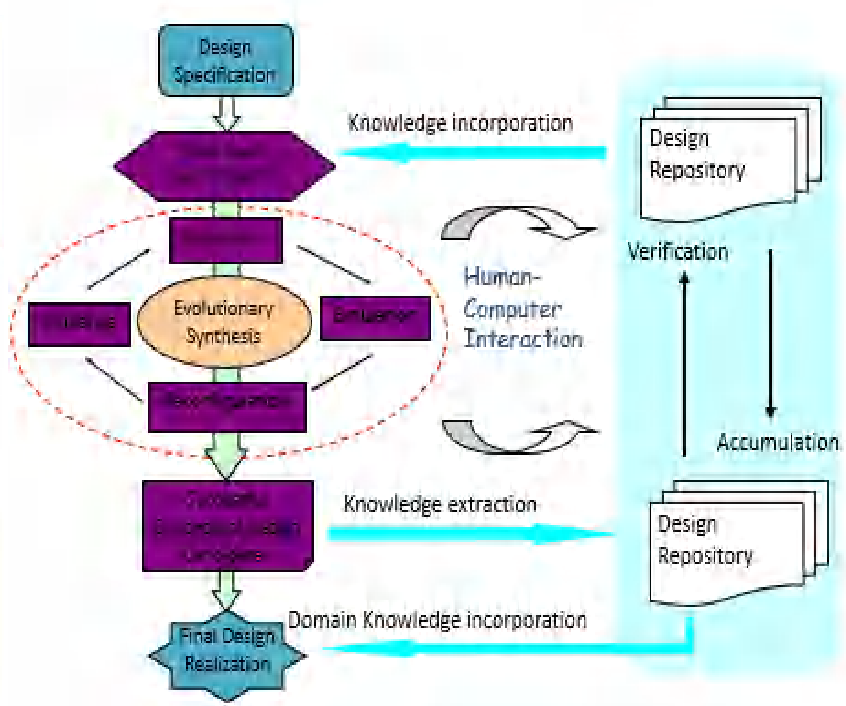

The framework of design automation.

- Design automation is a crucial branch of automation of knowledge work. Conducting research on Robotic Design Automation (RDA) is vital for enhancing the core competitiveness of China's robotic industry.
- Developing a design automation method that can continuously and systematically improve the performance of robotic designs holds vital importance for the future development of China’s robotic industry.

IRB 1410

IRB 1600

IRB 2400

ABB focuses on the research of Design Automation of Robotic Systems, and has been collaborating with Linkoping University for a long time.

research team and offering support on numerous occasions. I am very thankful of the great support we have had from ABB resulting in the fruitful cooperation we see today. I cannot imagine such a successful collaboration without the tireless efforts of Dr. Xiaolong Feng from ABB Corporate Research, whom I also would like to thank for

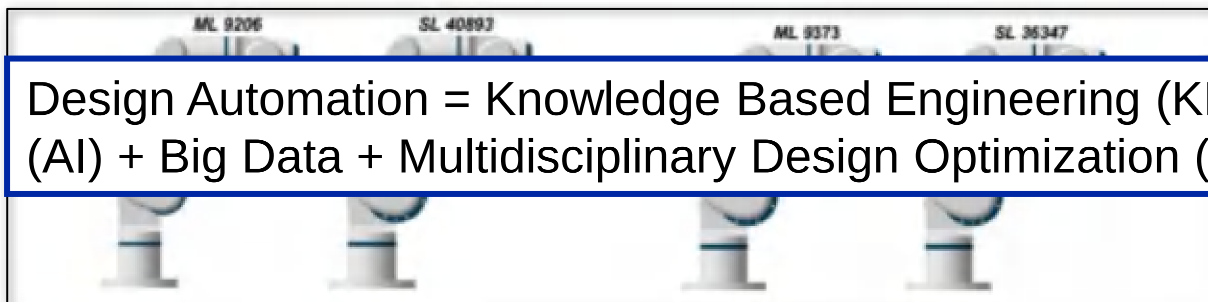

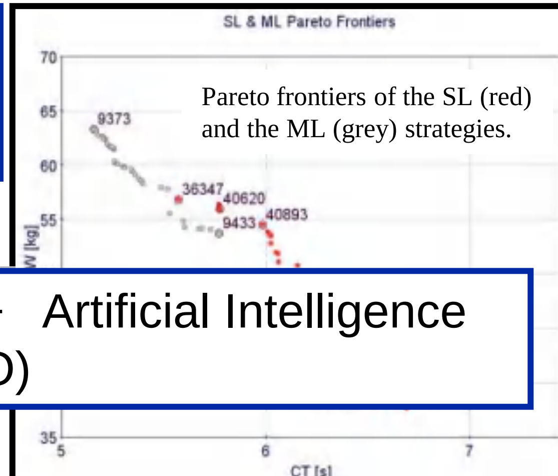

Pareto frontiers of the SL (red) and the ML (grey) strategies.

Design Automation = Knowledge Based Engineering (KBE)+ Artificial Intelligence (AI) + Big Data + Multidisciplinary Design Optimization (MDO)

Tarkian M. **Design** Reuse and **Automation**: On High Level CAD Modeling for Multidisciplinary Design and Optimization[J]. 2009.
Tarkian M. **Design Automation** for Multidisciplinary Optimization: A High Level CAD Template Approach[J]. 2012.

nature

Lipson H, Pollack J B. **Automatic design and manufacture of robotic lifeforms**[J]. ***Nature***, 2000, 406(6799): 974-978.
Zykov V, Mytilinaios E, Adams B, , Lipson H. **Self-reproducing machines**[J]. ***Nature***, 2005, 435(7038): 163-164.

Automatic design and manufacture of robotic lifefo

Hod Lipson & Jordan B. Pollack

Prof. Hod Lipson used Evolutionary Computing to first design robotic systems automatically in computer, and then made prototypes of the robots with 3D printing, thus realizing the concept of 'using a machine to design and make machines'.

teller machines. Here we report the results of a combined computational and experimental approach in which simple electromechanical systems are evolved through simulations from basic building blocks (bars, actuators and artificial neurons); the 'fittest' machines (defined by their locomotive ability) are then fabricated robotically using rapid manufacturing technology. We thus achieve autonomy of design and construction using evolution in a 'limited universe' physical simulation coupled to automatic fabrication.

Prof. Hod Lipson presented a more general research question as: can we automatically design a mechatronic/robotic system than can satisfy predefined design specifications using LEGO-like building blocks?

Self-reproducing machines

Fig. 2 Basic module, with an illustration of its internal actuation mechanism

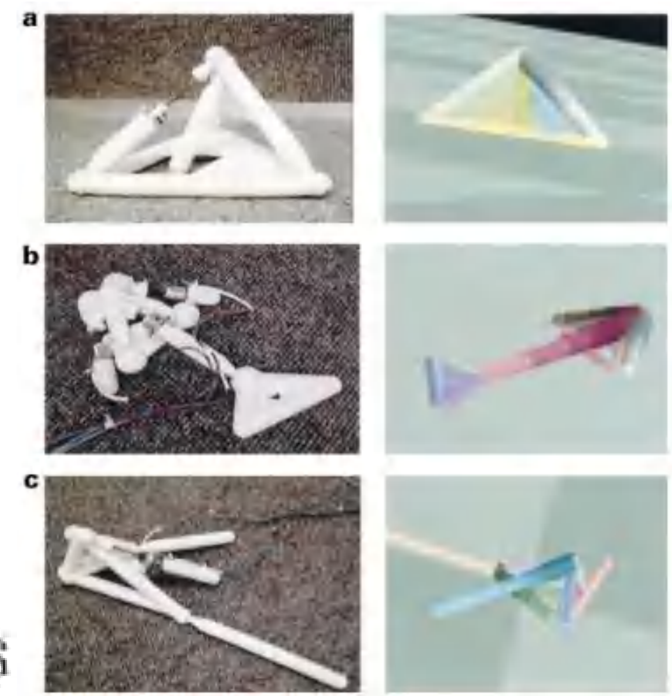

Fig. 1 Three resulting robots. Real robots (left); simulated robots (right)

The Director of BEACON Center, Prof. Erik Goodman and his team has made breakthrough research work in the field of mechatronic design automation.

…s paper presents an approach to engineering design of mixed-domain dynamic systems. The approach aims at …-level design and has two key features: first, it generates engineering designs that satisfy predefined specifications in an automatic manner; second, it can design systems belonging to different or mixed physical domains, such as electrical, mechanical, hydraulic, pneumatic, thermal systems and/or a mixture of them. Two important tools are used

Prof. Erik Goodman and his team developed a method called BGGP combining the capability of Bond Graph and Genetic Programming, and automatically designed a large variety of generic mechatronic systems.

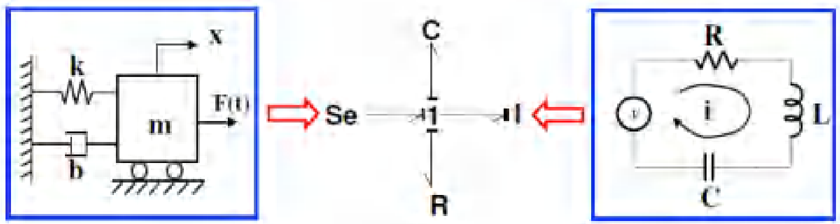

Fig. 3 Bond Graphs Representation of Mixed-Domain Systems

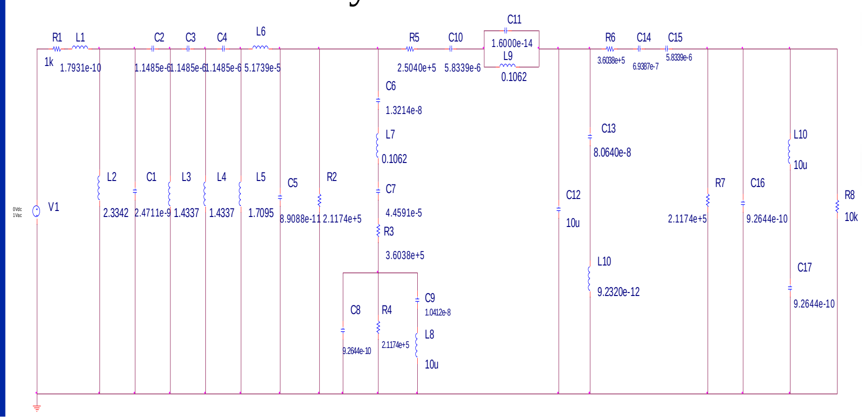

Fig. 4 Electric circuit for the evolved high-pass filter

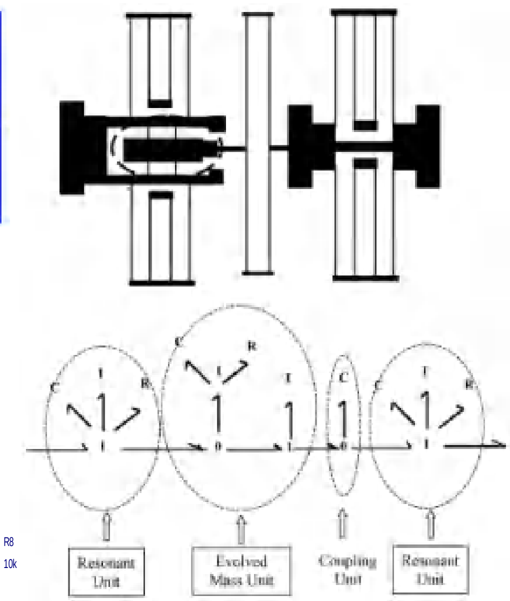

Fig. 5 A novel topology of MEM filter and its bond graph representation

Fan, Z., Seo, K., Hu, J., Goodman, E. D., & Rosenberg, R. C. (2004). A novel evolutionary engineering design approach for mixed-domain systems. *Engineering Optimization*, *36*(2), 127-147.

Prof. Clarence D. Silva （A Tier-I Research Chair in Mechatronics in Canada） and his team from UBC followed the work in my 2004 dissertation, and published another PhD dissertation in 2007, which extends the work of BGGP from treating only linear systems to nonlinear ones.

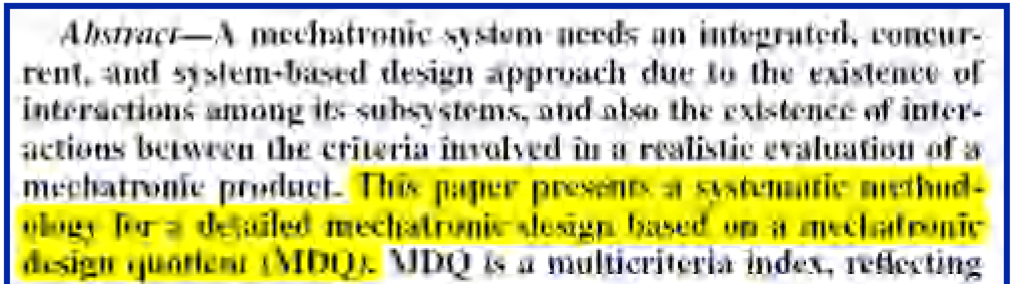
Abstract—A mechatronic system needs an integrated, concurrent, and system-based design approach due to the existence of interactions among its subsystems, and also the existence of interactions between the criteria involved in a realistic evaluation of a mechatronic product. This paper presents a systematic methodology for a detailed mechatronic design based on a mechatronic design quotient (MDQ). MDQ is a multicriteria index, reflecting

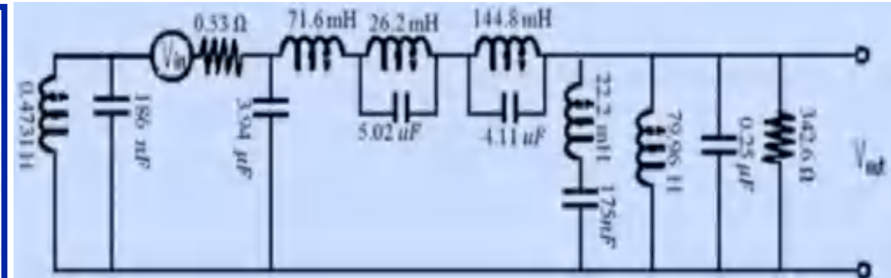

Figure 6 Evolved low-pass filter

Prof. Clarence D. Silva and his team also proposed the concept of MDQ (Mechatronic Design Quotient), so that BGGP or other MDA methods can now address design problems with multiple design objectives and constraints.

Figure 7 MDQ attributes

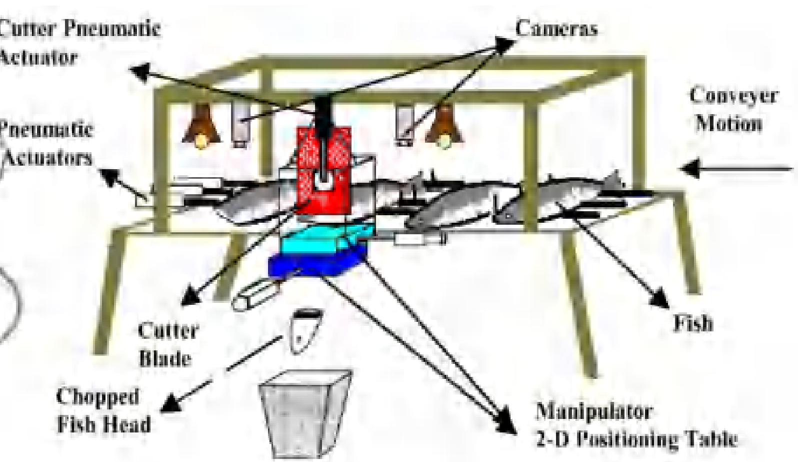

Figure 8 Fish cutting machine

Behbahani S, **de Silva C W**. System-based and concurrent design of a smart mechatronic system using the concept of mechatronic design quotient (MDQ)[J]. ***Mechatronics, IEEE/ASME Transactions on***, 2008, 13(1): 14-21. （**SCI, IF=3.851**）

We have continued to make groundbreaking progress in the area of **design automation of mechatronic systems for about 20 years**

The equivalent representation of the continuous controller is given by the bond graph, and the controlled plant and the controller are **designed in parallel** by genetic programming and co-evolution algorithms.

Vehicle Suspension Controller-Plant CoDesign

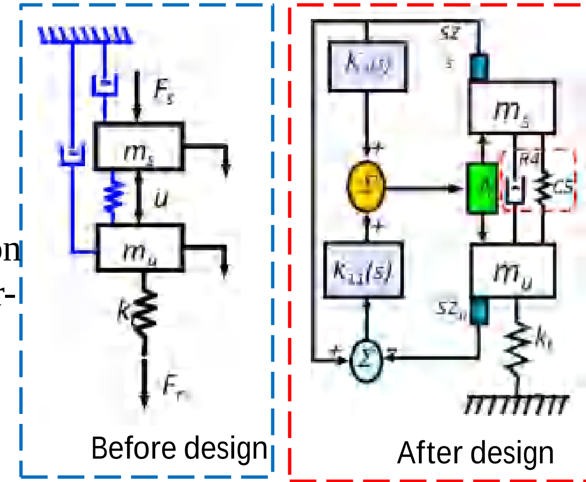

In order to overcome the limitation that the bond graph can only represent the **continuous** controller, a **model predictive controller** is used to represent a **discrete logic controller**, and the controller and the controlled plant are designed in parallel in an automatic manner.

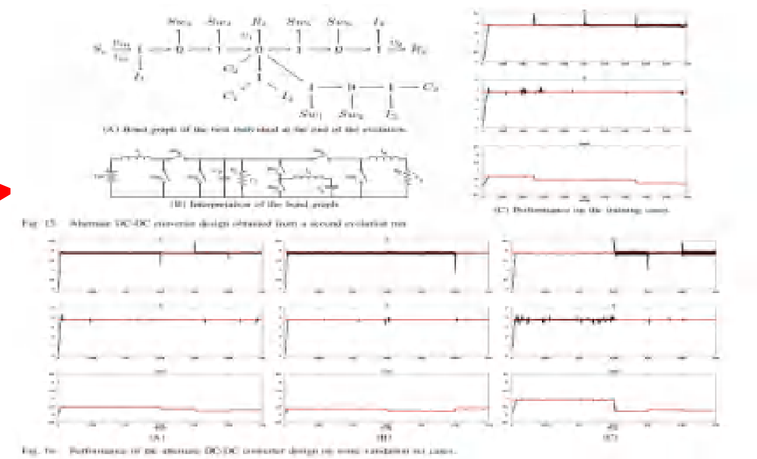

1. Analysis and multi-objective optimization of a kind of teaching manipulator. ***Swarm and Evolutionary Computation***, 2019, 50: 100554.
2. Evolutionary design of discrete controllers for hybrid mechatronic systems. ***International Journal of Systems Science***, 46(2): 303-316, 2015.
3. Evolutionary design of both topologies and parameters of a hybrid dynamical system. ***IEEE Transactions on Evolutionary Computation***, 16(3):391–405, 2012.
4. Cooperative body-brain co-evolutionary synthesis of mechatronic systems. ***Artificial Intelligence for Engineering Design, Analysis and Manufacturing***, 22(3):219–234, 2008.
5. Knowledge interaction with genetic Programming in mechatronic systems design using bond graph. ***IEEE Transactions on Systems, Man and Cybernetics***, 35(2):172-182, 2005.

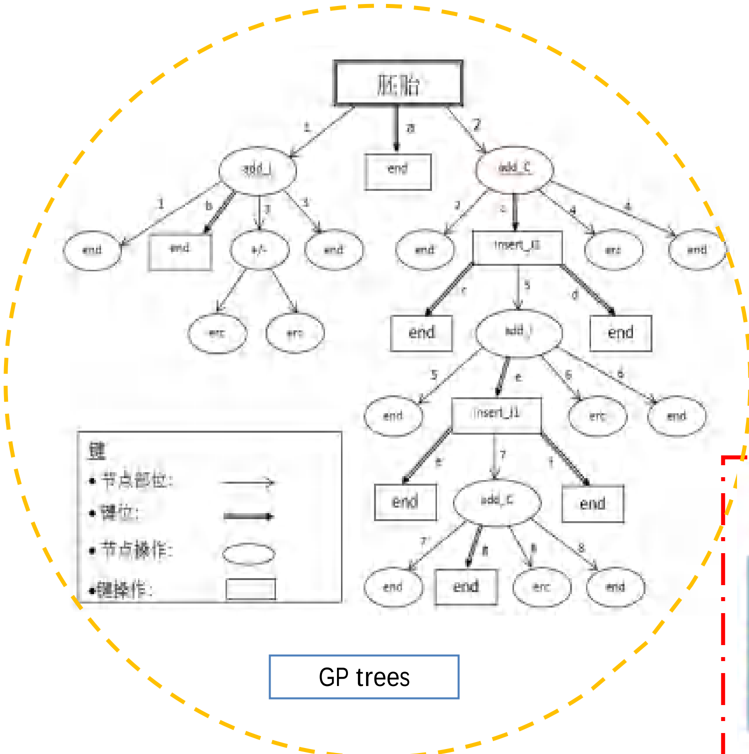

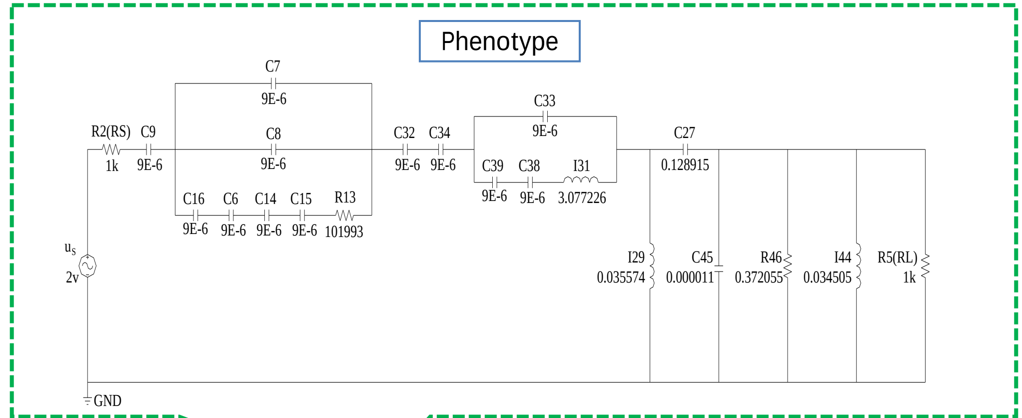

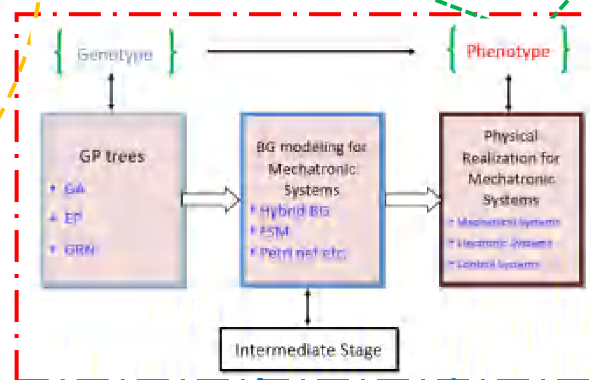

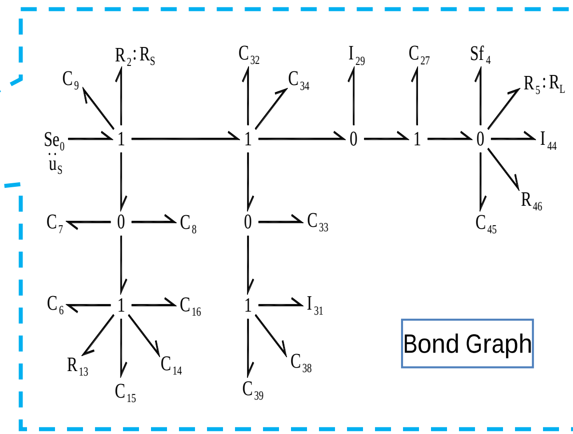

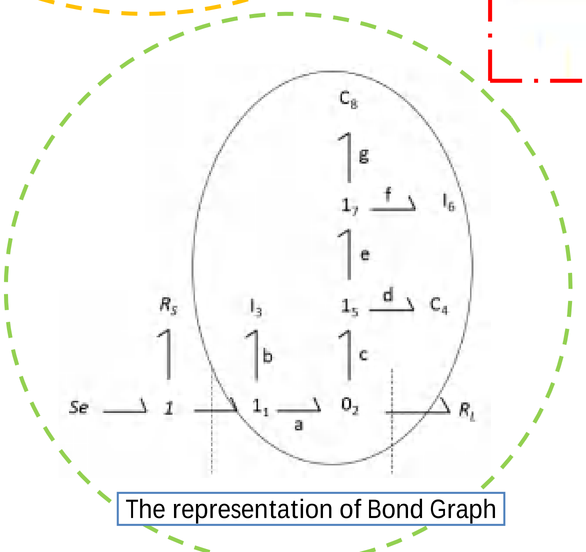

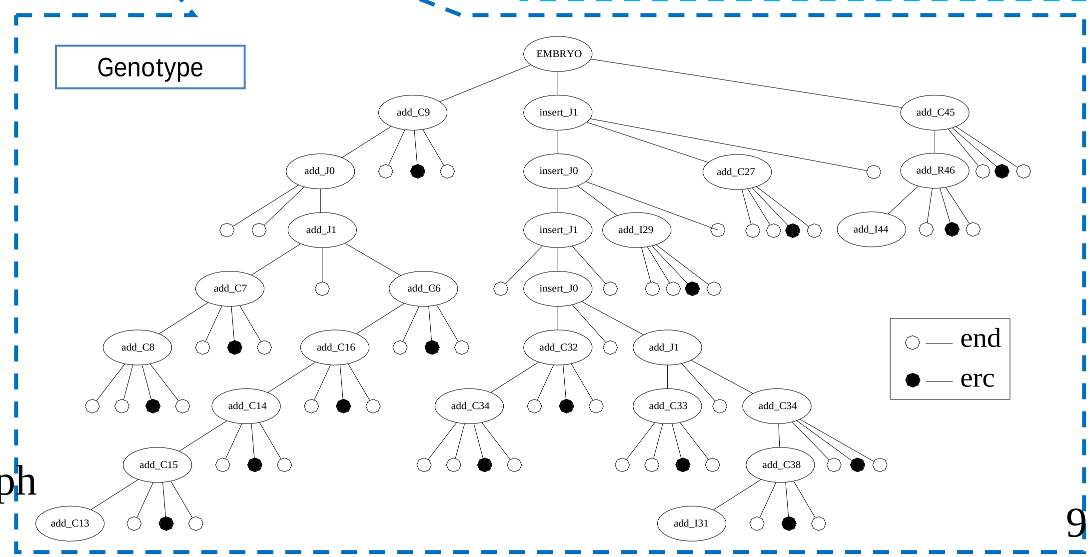

The design process by using GP and Bond Graph

Industrial Design Software for Intelligent Robots

汕頭大學
SHANTOU UNIVERSITY

- Our preliminary achievements have been integrated into the HEEDS software, which has now been acquired by Siemens and incorporated into its PLM software.
- The proposed design automation method incorporates multi-view modeling for more efficient simultaneous robot topology and parameter design, and more advanced constrained multi-objective optimization algorithms, thereby enhancing the forward design capabilities for robotic systems.

Definition → Simulation → Evaluation

Traditional method

Input: design variables

simulation models

Output: design performance

Does it meet the design objectives?

Iteration

Design automation methods

Input: Desired performance

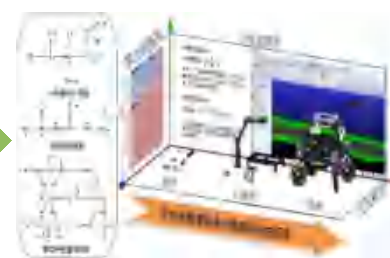

Multi-angle modeling

Output: Parallel optimization of structures and parameters

Faster and better results

《机器人设计自动化平台V1.0》软件著作权登记号：2018SR212300

A difficulty adjustable and scalable constrained multi-objective test problem toolkit has been proposed.

- We have defined the difficulty types of constraints for the first time and proposed three primary difficult categories: diversity hardness, feasibility hardness, and convergence hardness. These three primary types can be freely combined.

1. Constraint on shape functions

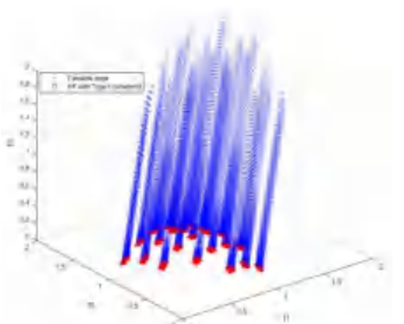

$$\Phi(x_{1:m-1}) \geq 0$$

2. Constraint on distance functions

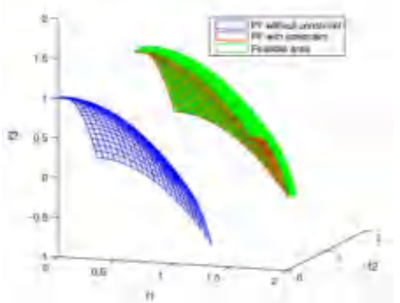

$$\Psi(x_{1:m-1}, x_{m:n}) \geq 0$$

3. Constraint on objective functions

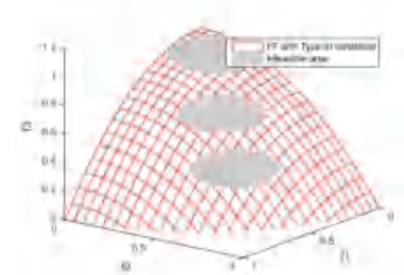

$$\Theta(f_{1:m}) \geq 0$$

Three Difficulty Types

- Diversity-Hardness
- Feasibility-Hardness
- Convergence-Hardness

DAS-CMOPs are considered by international peers to be a very important contribution to advancing research in constrained multi-objective evolutionary optimization.

Fan Z, Li W, Cai X, Li H, Wei C, Zhang Q, Deb K, Goodman E D. **Difficulty adjustable and scalable constrained multi-objective test problem toolkit**[J]. ***Evolutionary Computation***, 2020, 28(3):339-378. (SCI, IF= 6.8, Computer Science Q1**, 134 citations on Google Scholar.**)

Design Automation of Intelligent Robots

汕頭大學 SHANTOU UNIVERSITY

We proposed the push and pull search (PPS) framework, which guides the search first to the unconstrained Pareto front, and then from the unconstrained Pareto front back to the constrained one.

- Old Perspective (incorrect): Researchers treats all infeasible regions equally.
- New Perspective: We focus only on the few infeasible regions that intersect with the true Pareto front.

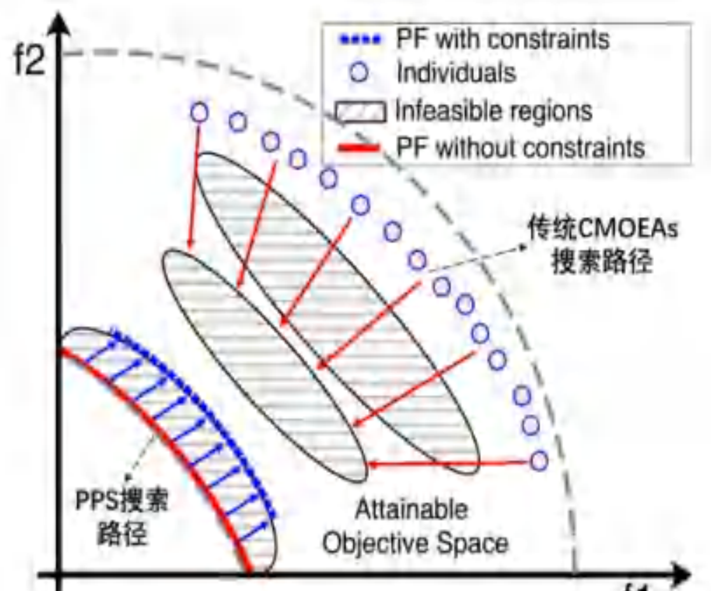

The framework of PPS

The teaching manipulator using the PPS algorithm outperformed NSGA-II by more than 2.5 times.

Fan Z, Li W, Cai X, Li H, Wei C, Zhang Q, Deb K, Goodman E D. **Push and pull search for solving constrained multi-objective optimization problems**[J]. ***Swarm and Evolutionary Computation***, 2019, 44: 665-679. (SCI, IF = 10, Artificial Intelligence Q1, **254 citations on Google Scholar, ESI highly cited paper.**)

Design Automation of Intelligent Robots

汕頭大學 SHANTOU UNIVERSITY

The integrated design automation of “Body-Brain-Eye” for intelligent robots

Morphology Model


机械臂


气源模块


运动底盘

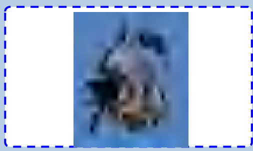
执行末端


视觉模块


控制柜

Design Automation Platform

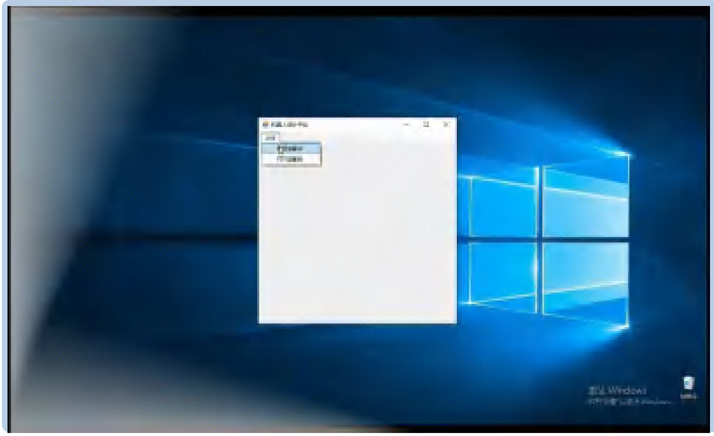

Pipeline Plugging Robot

Visual System


可见光图像

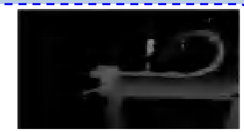
热成像图像

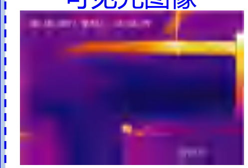
深度图像


末端摄像头图像


识别与定位

Design Automation of Intelligent Robots

We have developed a large variety of intelligent robot systems using the design automation method.

Pipeline Plugging Robot
ZL201920176692.3

Pavement Crack Detection Robot
ZL201811653343.2

Power Plant Surveillance Robot
ZL201610865308.1

Teaching Manipulator
ZL201721096302.9

Hexapod Robot
ZL201310136996.4

Snake-like Robot
ZL201310136949.X

Design Automation of Intelligent Robots

汕頭大學
SHANTOU UNIVERSITY

- Guided by the design automation method, we have developed a pipeline plugging robot, a pavement crack detection robot, a power plant surveillance robot, a teaching manipulator, a hexapod robot, and a snake-like robot. Based on these achievements, we were awarded the 2019 China Industry-University-Research Collaboration Innovation Award.

Pipeline Plugging Robot
ZL201920176692.3

Pavement Crack Detection Robot
ZL201811653343.2

Power Plant Surveillance Robot
ZL201610865308.1

Teaching Manipulator
ZL201721096302.9

Hexapod Robot
ZL201310136996.4

Snake-like Robot
ZL201310136949.X

Design automation of two mobile manipulator robots

- many robotic systems have important vision modules, which become increasingly indespensible in modern applications.

《机器人设计自动化平台V1.0》软件著作权登记号：2018SR212300

一种用于在线带压堵漏的复合型机器人. 实用新型 专利号：ZL201921611044.2

一种自主移动机器人平台用控制系统、方法及装置，发明专利 专利号： ZL201610865308.1

Design Automation for Vision Systems

汕頭大學 SHANTOU UNIVERSITY

- Manually designing CNN models to capture retinal vessels in fundus images is a well-known challenge requiring extensive empirical knowledge.
- Research groups across the world are competing to find a best-performing model.
- However, we propose to use a design automation method to outwit human competitors.

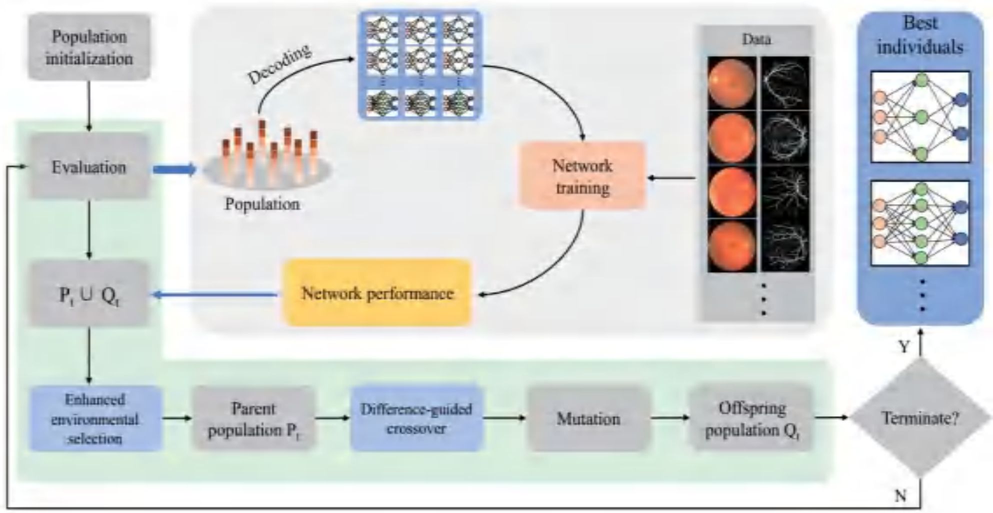

Fig. 4. The overall framework of the proposed method.

- We devised a condensed but flexible search space based on a U-shaped encoder-decoder, for the method called Genetic U-Net simultaneously optimizing the structures and parameters.
- The Genetic U-Net not only has higher detection performance than the manually designed models, but also fewer network parameters, outforming all reported SOTA methods.

基于进化神经架构搜索的眼底图像视网膜血管分割方法。专利号：ZL 202011172307.1

Wei J., Zhu G., **Fan Z.***, Liu J., Rong Y., Chen X. **Genetic U-Net: automatically designing deep networks using the genetic algorithm for retinal vessel segmentation**[J]. ***IEEE Transactions on Medical Imaging***, 41(2), 292-307. (SCI 1 区 TOP期刊, IF = 10.048)

"Body"— Design automation for Morphologies

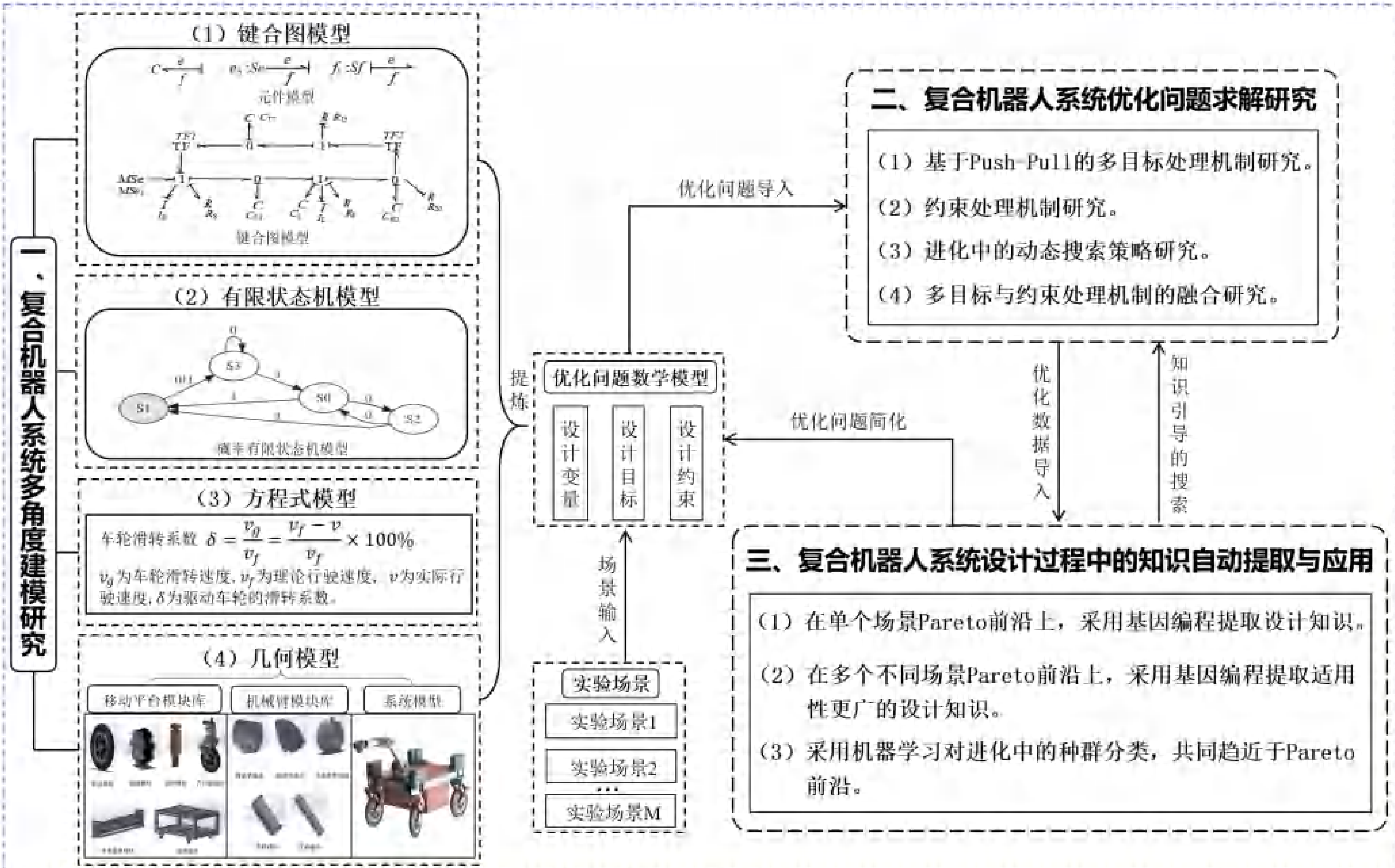

"Body"— Design automation for Morphologies

"Eye" - Design Automation for Vision Systems

汕頭大學 SHANTOU UNIVERSITY

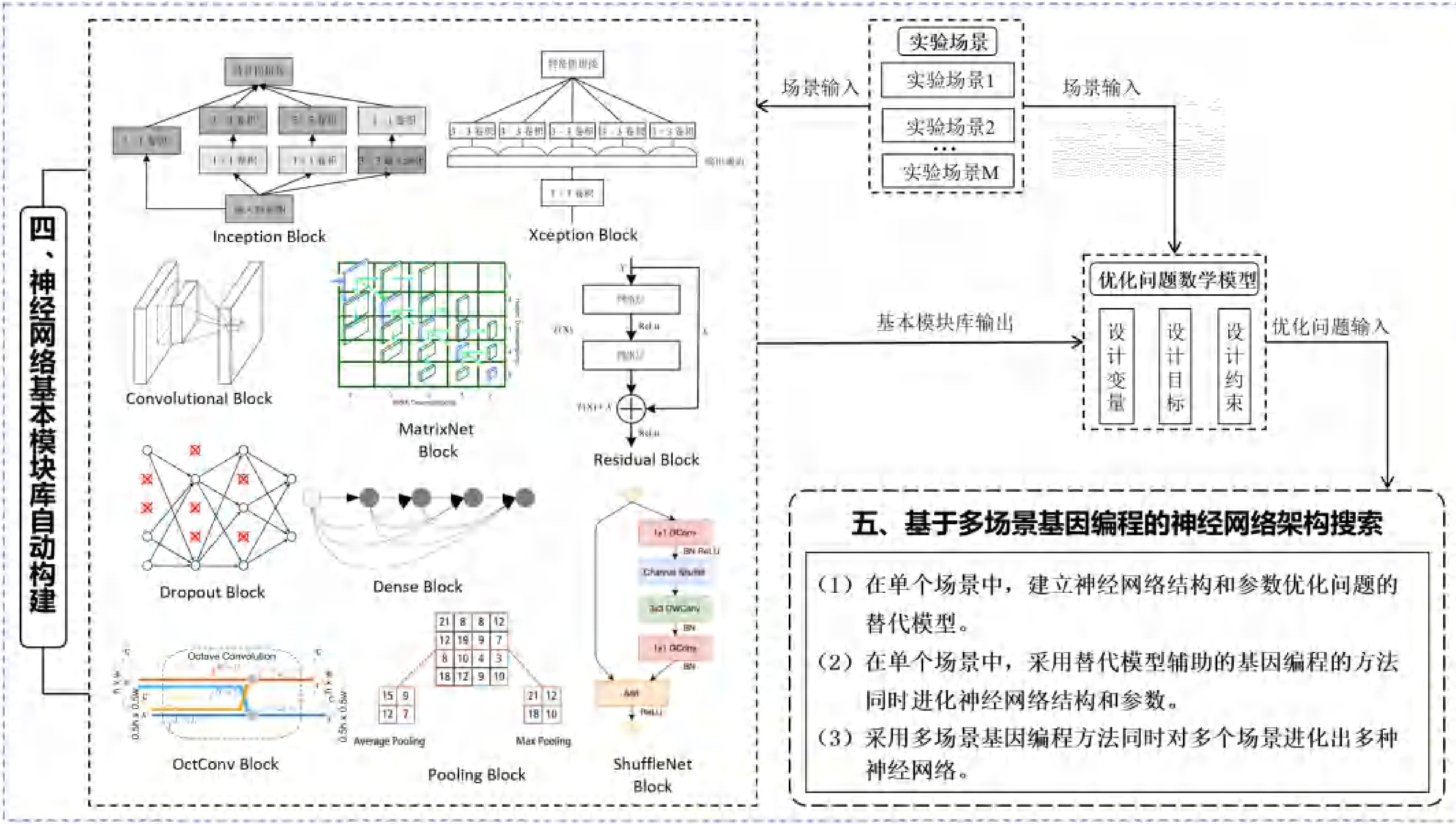

"Eye" - Design Automation for Vision Systems

Intelligent Design of Deep Neural Networks

汕頭大學 SHANTOU UNIVERSITY

Search Space and Encoding

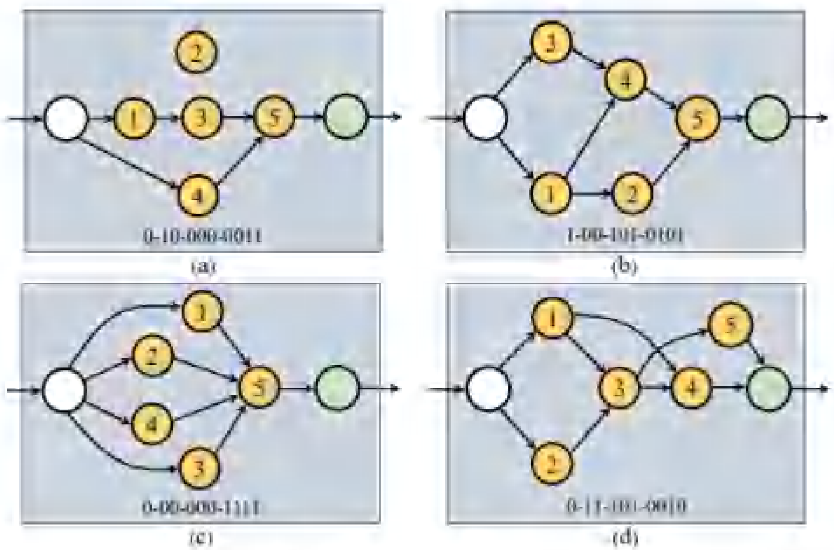

Fig. 2. Four encoding examples of the inter-node connections in a block. The white node, the green node, and the yellow nodes represent the default input node, the default output node, and the intermediate nodes ($node_1, node_2, ..., node_K$ ($K = 5$ in these four examples)). The numbers in the intermediate nodes indicate their orders for encoding. There is a possible maximum of seven nodes in a block in these four examples, and binary encoding with 10 bits represents the connections between nodes in a block. See Section III-A.2 for detailed descriptions of the encoding schemes of the inter-nodal connections.

TABLE I

THE OPERATION SEQUENCES FOR THE NODES.

ID	Operation sequence	ID	Operation sequence
0	3×3 conv → ReLU	8	ReLU → 3×3 conv
1	3×3 conv → Mish	9	Mish → 3×3 conv
2	3×3 conv → IN → ReLU	10	IN → ReLU → 3×3 conv
3	3×3 conv → IN → Mish	11	IN → Mish → 3×3 conv
4	5×5 conv → ReLU	12	ReLU → 5×5 conv
5	5×5 conv → Mish	13	Mish → 5×5 conv
6	5×5 conv → IN → ReLU	14	IN → ReLU → 5×5 conv
7	5×5 conv → IN → Mish	15	IN → Mish → 5×5 conv

IN represents the instance normalization, ReLU indicates Rectified Linear Unit, and Mish is a self-regularized non-monotonic neural activation function.

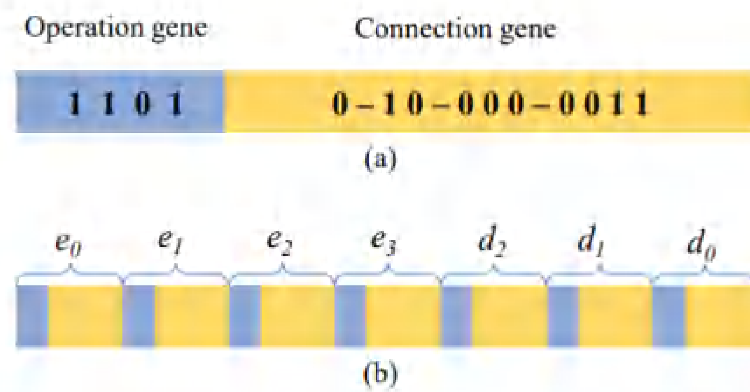

Fig 3 (a) A block gene; (b) Genotype of an architecture consisting of seven block genes.

Wei J., Zhu G., **Fan Z.***, Liu J., Rong Y., Chen X. **Genetic U-Net: automatically designing deep networks using the genetic algorithm for retinal vessel segmentation**[J]. ***IEEE Transactions on Medical Imaging***, 41(2), 292-307. (SCI 1 区 TOP期刊, IF = 10.048)

Search Space and Encoding

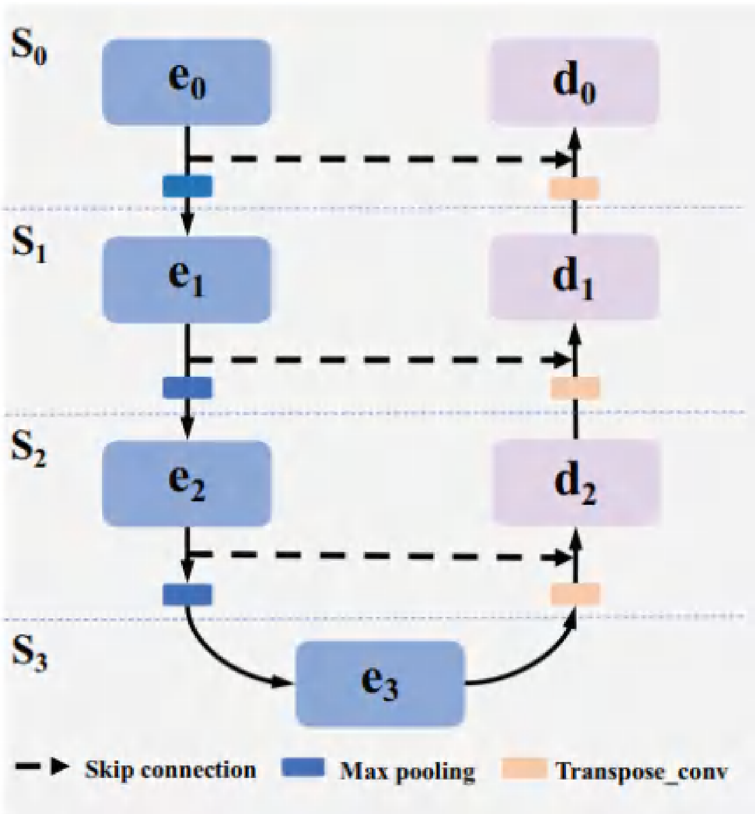

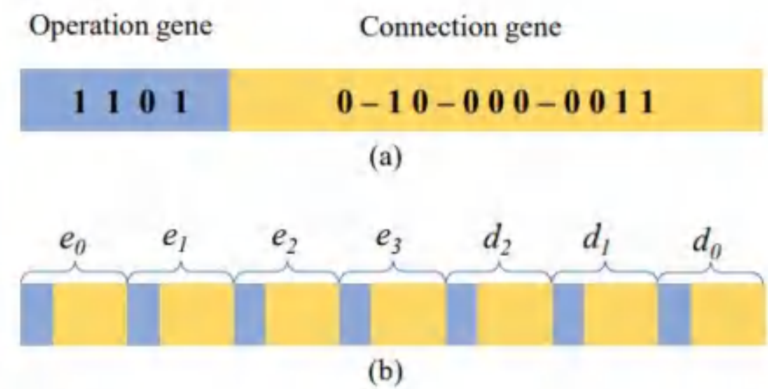

Fig. 3. (a) A block gene; (b) Genotype of an architecture consisting of seven block genes.

- **Most network architectures in this search space have fewer than 0.4 M parameters**

Wei J., Zhu G., **Fan Z.***, Liu J., Rong Y., Chen X. **Genetic U-Net: automatically designing deep networks using the genetic algorithm for retinal vessel segmentation**[J]. ***IEEE Transactions on Medical Imaging***, 41(2), 292-307. (SCI 1 区 TOP期刊, IF = 10.048)

- **Materials for Experiments**

Loss Function (Focal loss):

$$Loss = -\sum_{n=1}^{m} \left(\alpha y_n \left(1-\hat{y}_n\right)^{\omega} log\hat{y}_n + \left(1-\alpha\right)\left(1-y_n\right)\hat{y}_n^{\omega} log\left(1-\hat{y}_n\right)\right)$$

Datasets:

Dataset	Quantity	Resolution	training-testing split
DRIVE	40	565×584	20/20
STARE	20	700×605	leave one out
CHASE_DB1	28	999×960	20/8
HRF	45	3504×2336	15/30

Evaluation metrics:

Metrics	Description
ACC *(accuracy)*	$ACC = (TP + TN) / (TP + TN + FP + FN)$
SE *(sensitivity)*	$SE = TP / (TP + FN)$
SP *(specificity)*	$SP = TN / (TN + FP)$
$F1$ *(F1 score)*	$F1 = (2 \times TP) / (2 \times TP + FP + FN)$
$AUROC$	Area Under the ROC Curve.

Comparison with Existing Methods

TABLE IV

COMPARISON WITH EXISTING METHODS ON DRIVE DATASET.

Methods	Year	ACC	SE	SP	FI	AUROC	Params(M)
Vega *et al.* [17]	2015	0.9412	0.7444	0.9612	0.6884	N/A	N/A
Li *et al.** [18]	2015	0.9527	0.7569	0.9816	N/A	0.9738	N/A
Orlando *et al.** [14]	2016	N/A	0.7897	0.9684	0.7857	N/A	N/A
Fan and Mo [20]	2016	0.9612	0.7814	0.9788	N/A	N/A	N/A
Liskowski *et al.** [16]	2016	0.9535	0.7811	0.9807	N/A	0.9790	48.00
Mo and Zhang [19]	2017	0.9521	0.7779	0.9780	N/A	0.9782	7.63
Yan *et al.** [33]	2018	0.9542	0.7653	0.9818	N/A	0.9752	31.35
Alom *et al.** [24]	2019	0.9556	0.7792	0.9813	0.8171	0.9784	1.07
Jin *et al.** [8]	2019	0.9566	0.7963	0.9800	0.8237	0.9802	0.88
Bo Wang *et al.** [10]	2019	0.9567	0.7940	0.9816	0.8270	0.9772	N/A
Yicheng Wu *et al.* [22]	2019	0.9578	0.8038	0.9802	N/A	0.9821	1.70
Mou Lei *et al.* [9]	2019	0.9594	0.8126	0.9788	N/A	0.9796	56.03
CE-Net* [25]	2019	0.9545	0.8276	0.9735	0.8243	0.9794	15.28
CS^2-Net* [26]	2021	0.9553	0.8154	0.9757	0.8228	0.9784	8.91
Genetic U-Net w/ FOVs	-	0.9577	**0.8300**	0.9758	**0.8314**	**0.9823**	**0.27**
Genetic U-Net w/o FOVs	-	**0.9707**	**0.8300**	**0.9843**	**0.8314**	**0.9885**	**0.27**

TABLE VI

COMPARISON WITH EXISTING METHODS ON THE CHASE_DB1 DATASET.

Methods	Year	ACC	SE	SP	FI	AUROC
Li *et al.** [18]	2015	0.9581	0.7507	0.9793	N/A	0.9716
Fan and Mo [20]	2016	0.9573	0.7656	0.9704	N/A	N/A
Yan *et al.** [33]	2018	0.9610	0.7633	0.9809	N/A	0.9781
Alom *et al.** [24]	2019	0.9634	0.7756	0.9820	0.7928	0.9815
Bo Wang *et al.** [10]	2019	0.9661	0.8074	0.9821	0.8037	0.9812
Yicheng Wu *et al.* [22]	2019	0.9661	0.8132	0.9814	N/A	0.9860
CE-Net* [25]	2019	0.9641	0.8093	0.9797	0.8054	0.9834
CS^2-Net* [26]	2021	0.9651	0.8329	0.9784	0.8141	0.9851
Genetic U-Net w/ FOVs	-	**0.9667**	**0.8463**	0.9845	**0.8223**	**0.9880**
Genetic U-Net w/o FOVs	-	**0.9769**	**0.8463**	**0.9857**	**0.8223**	**0.9914**

TABLE VII

COMPARISON WITH EXISTING METHODS ON THE HRF DATASET.

Methods	Year	ACC	SE	SP	FI	AUROC
Orlando *et al.** [14]	2016	N/A	0.7794	0.9650	0.7341	N/A
Yan *et al.** [33]	2018	0.9437	0.7881	0.9592	N/A	N/A
Jin *et al.** [8]	2019	0.9651	0.7464	**0.9874**	N/A	0.9831
CE-Net* [25]	2019	0.9613	0.7805	0.9798	0.7895	0.9766
CS^2-Net* [26]	2021	0.9618	0.7890	0.9795	0.7935	0.9758
Genetic U-Net w/ FOVs	-	**0.9667**	**0.8220**	0.9818	**0.8179**	**0.9872**
Genetic U-Net w/o FOVs	-	**0.9715**	**0.8220**	0.9839	**0.8179**	**0.9891**

TABLE V

COMPARISON WITH EXISTING METHODS ON THE STARE DATASET.

Methods	Year	ACC	SE	SP	FI	AUROC
Vega *et al.* [17]	2015	0.9483	0.7019	0.9671	0.6614	N/A
Li *et al.** [18]	2015	0.9628	0.7726	0.9844	N/A	0.9879
Orlando *et al.** [14]	2017	N/A	0.7680	0.9738	0.7644	N/A
Fan and Mo [20]	2016	0.9654	0.7834	0.9799	N/A	N/A
Liskowski *et al.** [16]	2016	0.9566	0.7867	0.9754	N/A	0.9785
Mo and Zhang [19]	2018	0.9674	0.8147	0.9844	N/A	0.9885
Yan *et al.** [33]	2018	0.9612	0.7581	0.9846	N/A	0.9801
Alom *et al.** [24]	2019	0.9712	0.8292	0.9862	0.8475	0.9914
Jin *et al.** [8]	2019	0.9641	0.7595	0.9878	0.8143	0.9832
CE-Net* [25]	2019	0.9656	0.8406	0.9813	0.8363	0.9871
CS^2-Net* [26]	2021	0.9670	0.8396	0.9813	0.8420	0.9875
Genetic U-Net w/ FOVs	-	**0.9719**	**0.8658**	0.9846	**0.8630**	**0.9921**
Genetic U-Net w/o FOVs	-	**0.9792**	**0.8658**	**0.9886**	**0.8630**	**0.9942**

- **Visual Comparison**

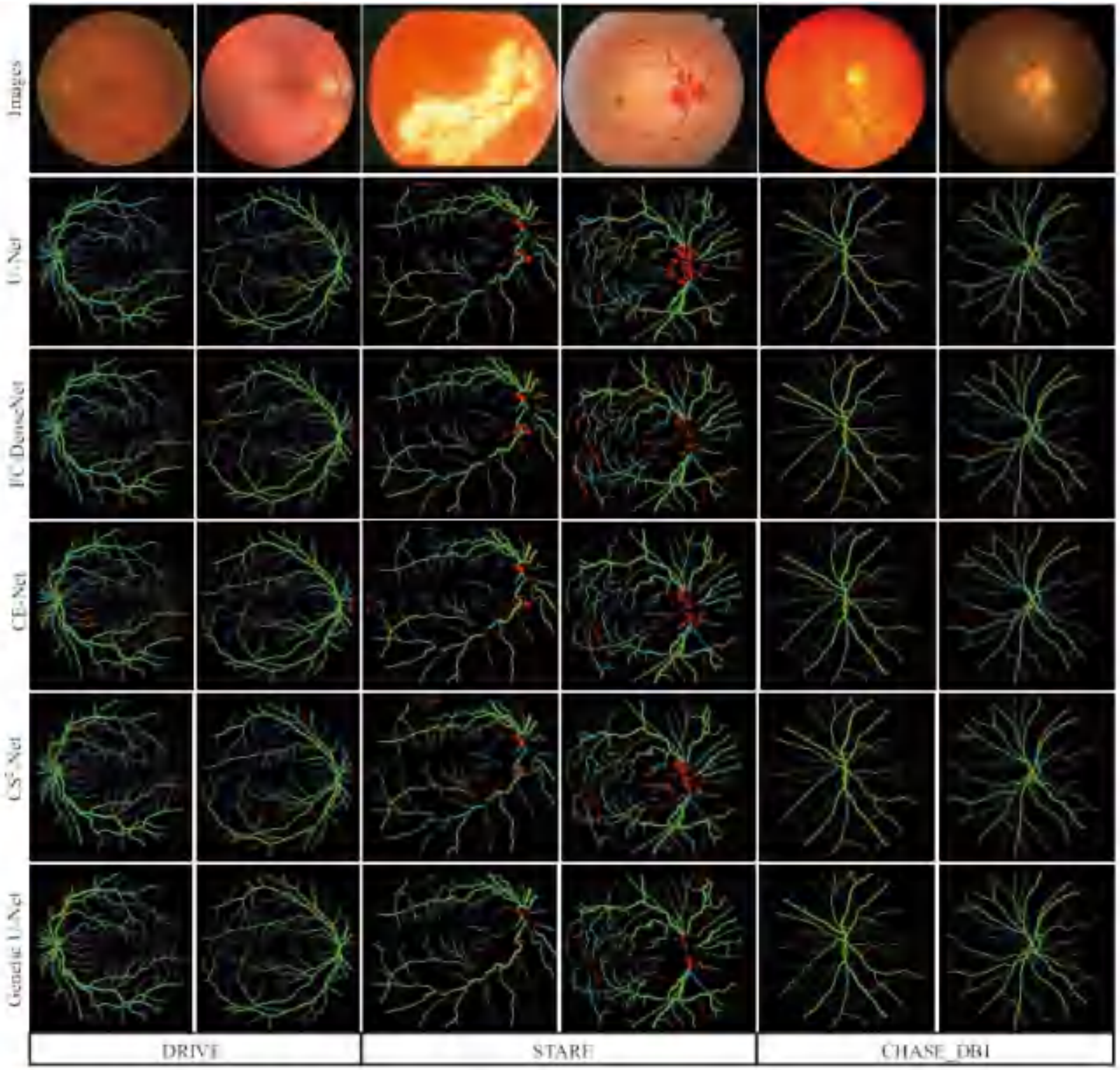

Fig. 5. Overall view visualization of the segmentation results. The green pixels indicate true positive, red pixels indicate false positive, and blue pixels indicate false negative.

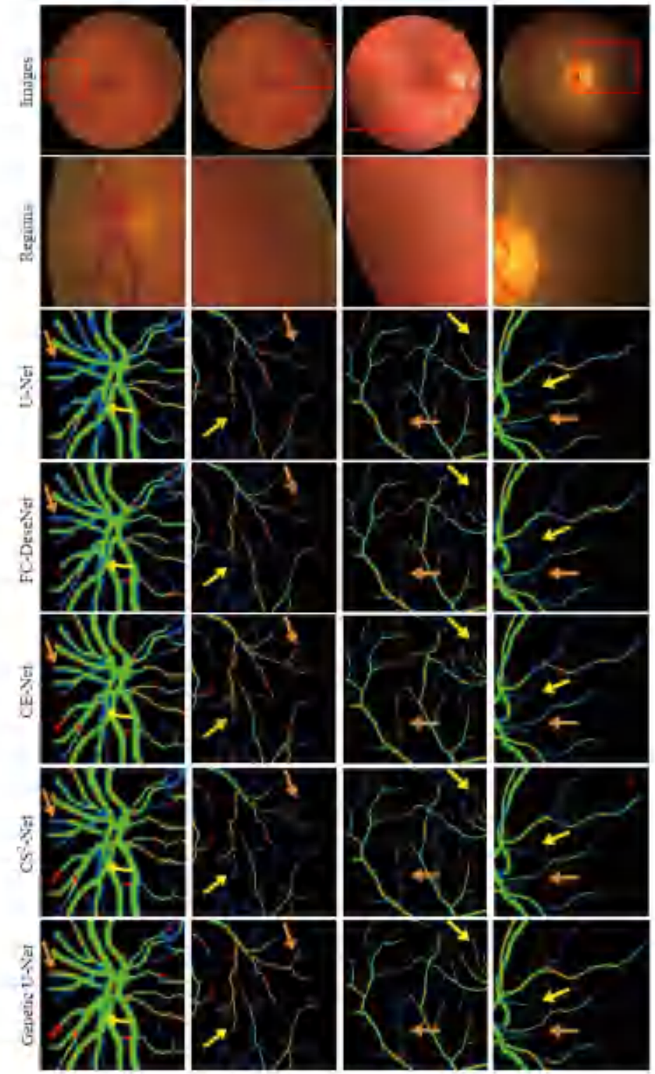

Fig. 6. Locally magnified view visualization of the segmentation results.

- **The found architecture**

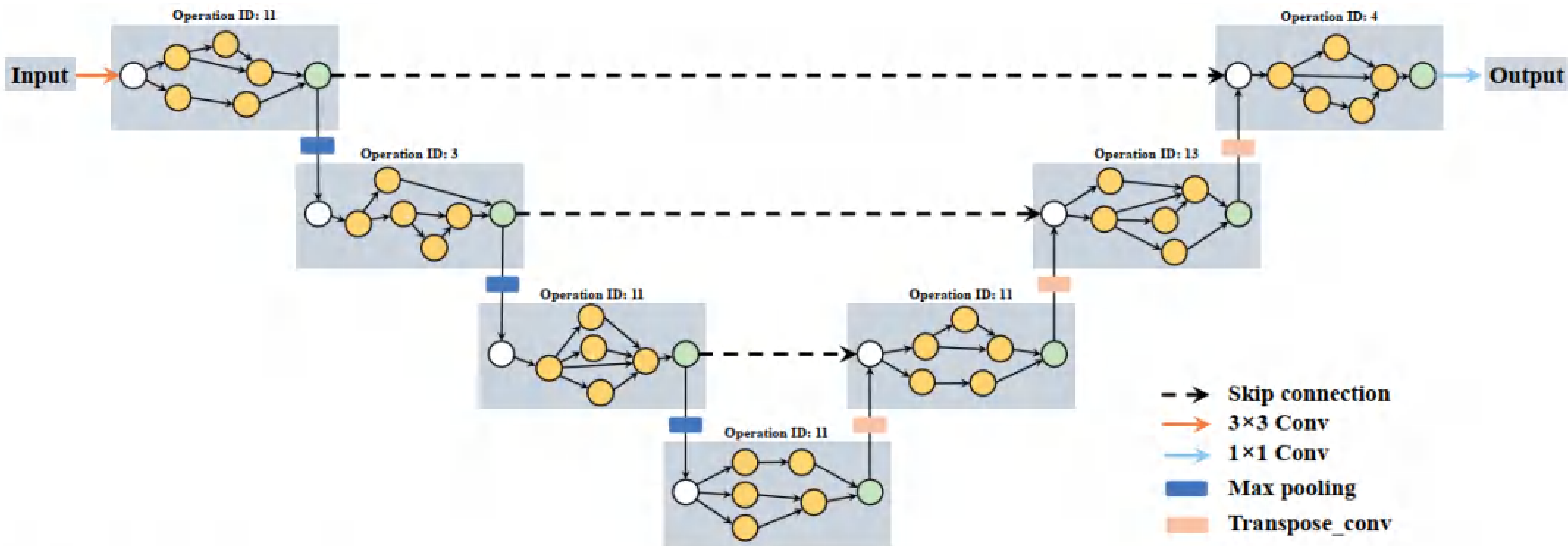

Fig. 12. The first best architecture.

- **The found architectures**

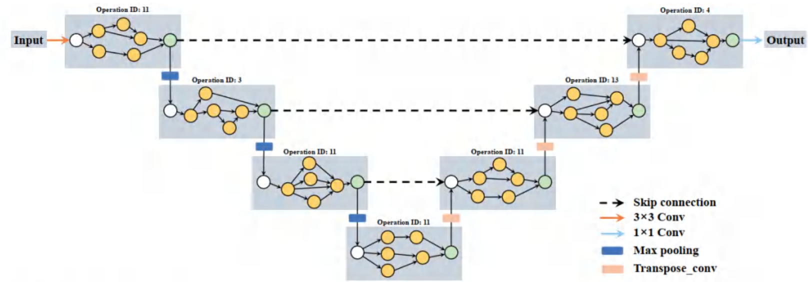

Fig. 12. The first best architecture.

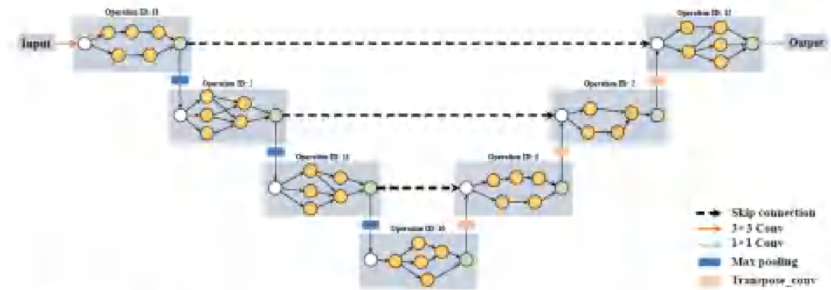

Fig. 13. The second best architecture.

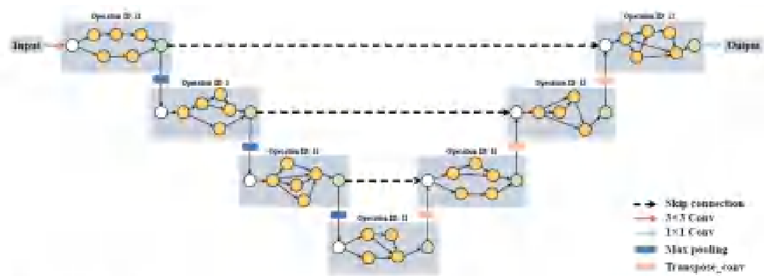

Fig. 14. The third best architecture.

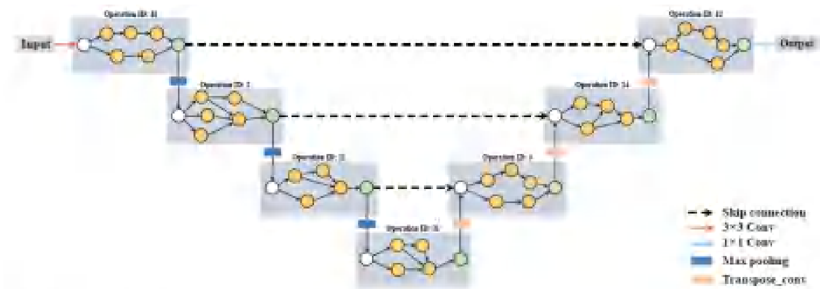

Fig. 15. The fourth best architecture.

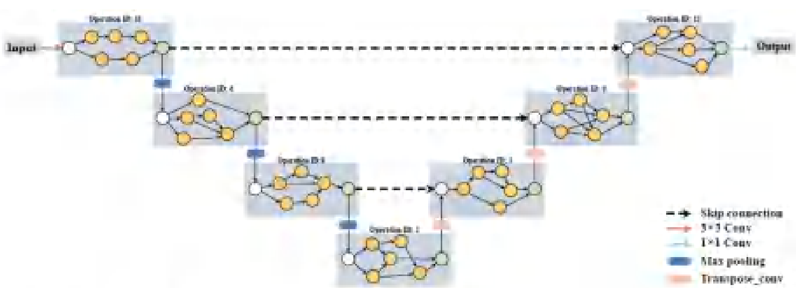

Fig. 16. The fifth best architecture.

- **Performance on Cell Boundary Segmentation**

TABLE XIII
COMPARISONS ON CELL MEMBRANE (BOUNDARY) SEGMENTATION.

Models	ACC	SE	SP	F1	AUROC
U-Net	0.9112	0.8179	0.9401	0.8097	0.9587
FC-Densenet	0.9132	0.8291	0.9361	0.8167	0.9627
CE-Net	0.9099	0.8253	0.9233	0.8161	0.9645
CS^2-Net	0.9109	0.8263	0.9272	0.8163	0.9634
Genetic U-Net	**0.9171**	**0.8376**	**0.9446**	**0.8212**	**0.9666**

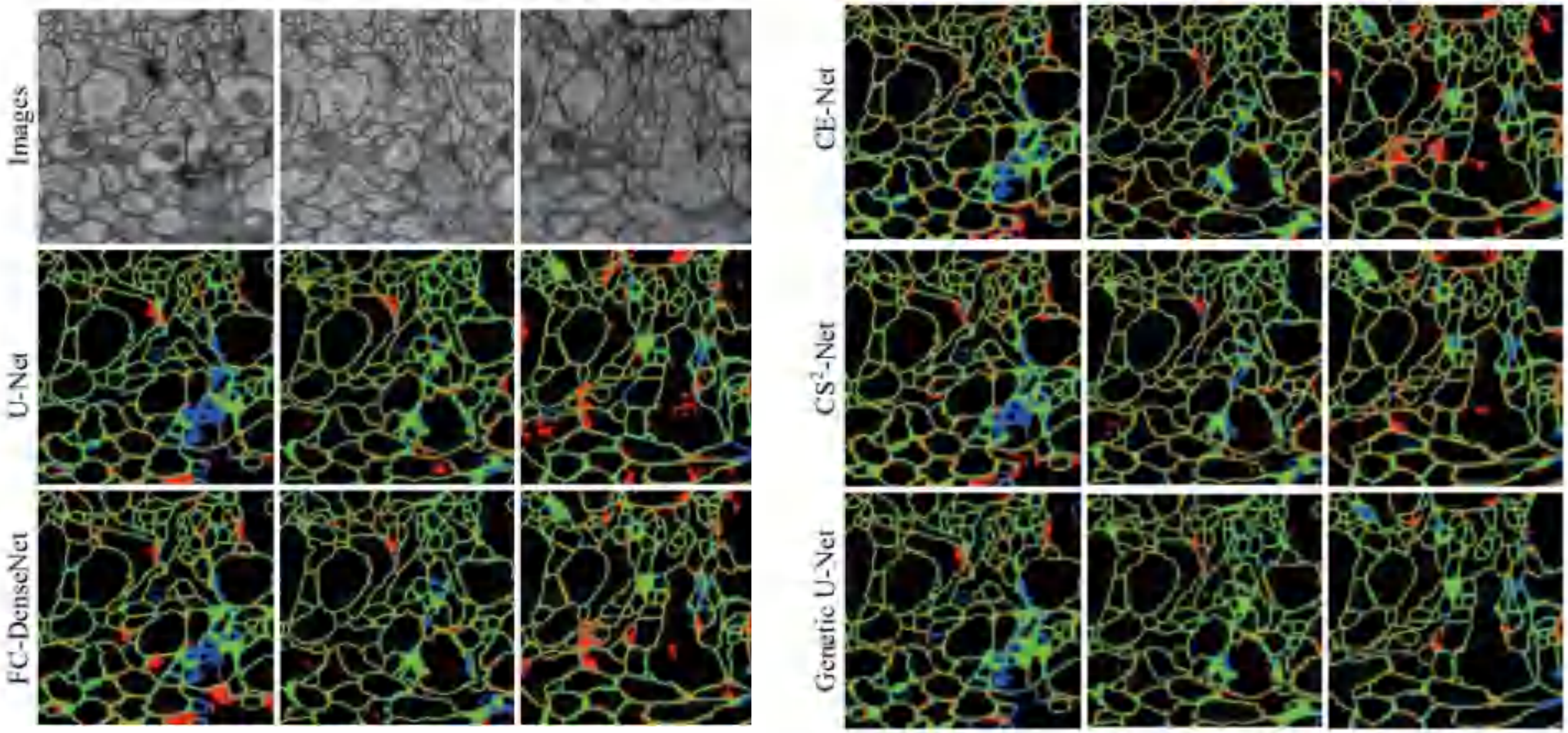

Intelligent Design of Deep Neural Networks

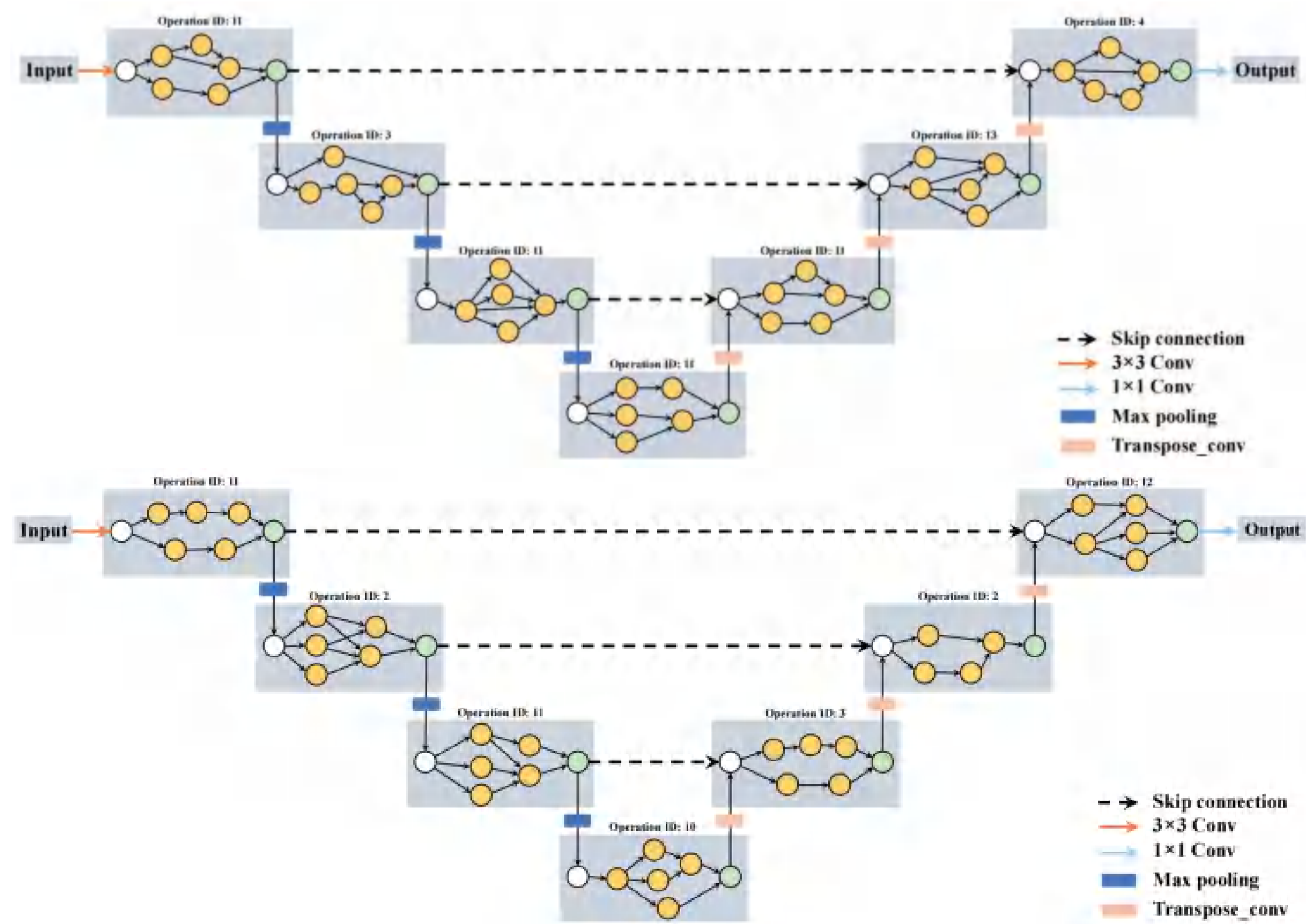

Fig 1. Deep neural network optimized by Genetic U-Net

Wei J., Zhu G., **Fan Z.***, Liu J., Rong Y., Chen X. **Genetic U-Net: automatically designing deep networks using the genetic algorithm for retinal vessel segmentation**[J]. ***IEEE Transactions on Medical Imaging***, 41(2), 292-307. (SCI 1 区 TOP期刊, IF = 10.048)

Intelligent Design of Deep Neural Networks

汕頭大學 SHANTOU UNIVERSITY

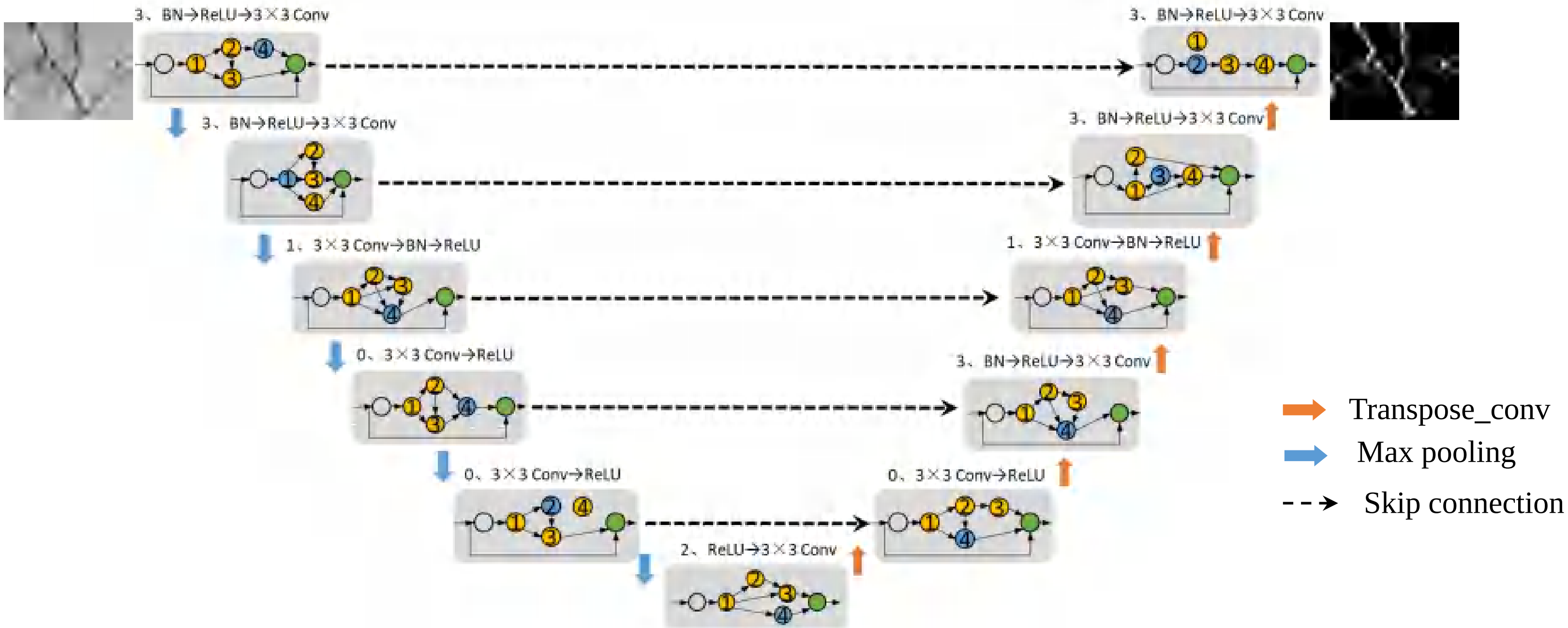

Fig 1. Deep neural network optimized by particle swarm optimization

CFD						
Method	**Re**	**Pr**	**F1**	**IOU**	**Flops**	**Param**
U-Net [MICCAI 2015]	0.9195	0.9059	0.9116	0.8687	1.2814	31.0317
DeepCrack_Zou [TIP 2018]	0.8417	0.8461	0.8404	0.7506	3.2064	30.9050
DeepCrack_Liu [2019]	0.8962	0.8891	0.8903	0.8314	0.4716	14.7204
FPHBN [Neurocomputing 2019]	0.9145	0.9040	0.9047	0.8545	1.4790	34.9191
BiSeNet V2 [IJCV 2021]	0.9186	0.8764	0.8955	0.8399	0.0756	3.6182
DMA-Net [TITS 2022]	0.9234	0.8898	0.8987	0.8451	0.5350	60.4619
Ours	**0.9310**	**0.9143**	**0.9204**	**0.8823**	**0.0742**	**0.2073**

Pavement Crack Detection Based on a Lightweight Encoder-Decoder Network

汕頭大學 SHANTOU UNIVERSITY

Combining the advantages of U-Net architecture, residual blocks and the hybrid attention mechanism, a lightweight encoder-decoder network (with only 0.57M model parameters) for road crack detection is proposed.

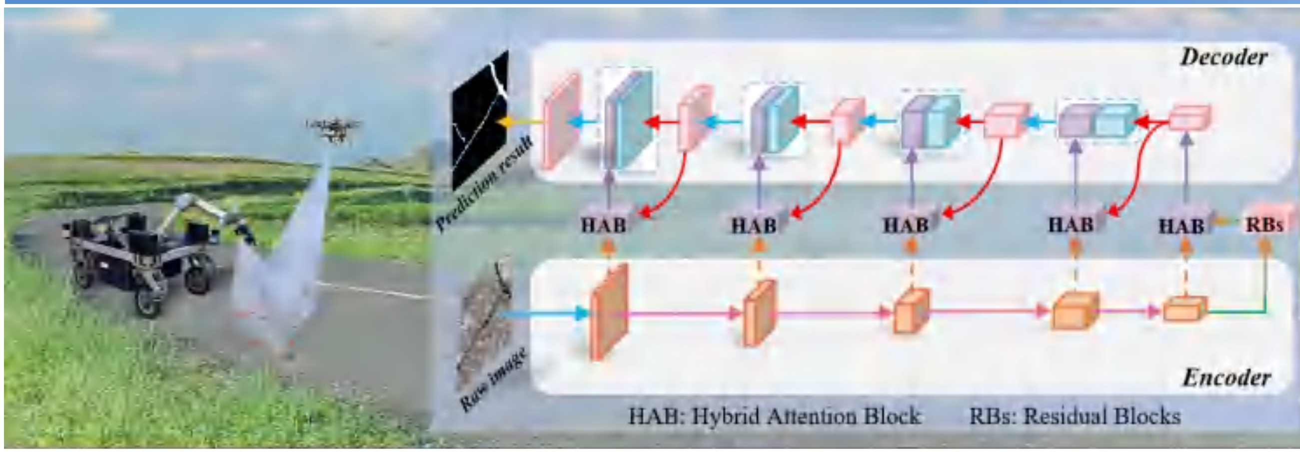

Existing methods are time-consuming and costly to train, and they are challenging to use for real-time crack detection on-site, especially under limited computing resources or environmental constraints.

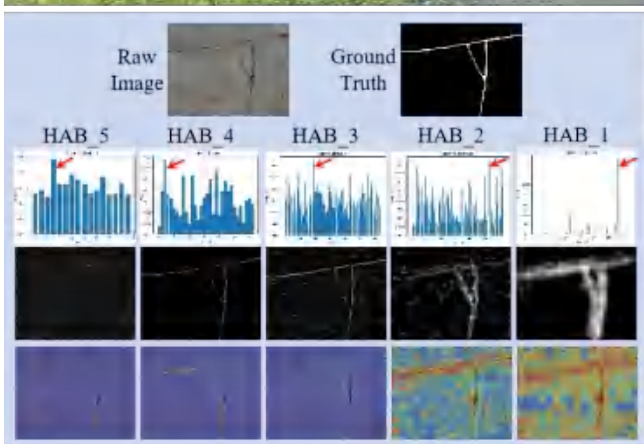

TABLE 8 Comparison of parameters and FLOPs of all models.

Models	Params	FLOPs
FCN [CVPR 2015]	18.64 M	239.46 G
U-Net [MICCAI 2015]	17.25 M	375.24 G
Attention U-Net [MIDL 2018]	34.88 M	624.72 G
DC_Zou [TIP 2018]	30.91 M	1283.64 G
DC_Liu [Neurocomputing 2019]	14.72 M	188.56 G
DMA-Net [TITS 2022]	60.46 M	212.12 G
AttentionCrackNet [CACAIE 2022]	23.47 M	329.02 G
RHACrackNet	1.67 M	21.6 G
RHACrackNet*	0.57 M	9.68 G

G. Zhu, J. Liu, **Z. Fan*,** D. Yuan, P. Ma, M. Wang*, W. Sheng, K. C. P. Wang. **A lightweight encoder–decoder network for automatic pavement crack detection**[J]. ***Computer-Aided Civil and Infrastructure Engineering***, 2023: 1–23. (SCI 1区TOP期刊， IF = 9.6)

Pavement Crack Detection Based on a Lightweight Encoder-Decoder Network

The proposed method is capable of detecting pavement cracks in real-time at 25 FPS.

Design Automation for Swarm Behavior Control

We employ the same design automation framework to achieve the automated design of swarm behavior coordination strategies.

- The proposed method can automatically generate gene regulatory networks for swarm behaviors to form entrapping patterns to encircle escaping targets in dynamic environments.

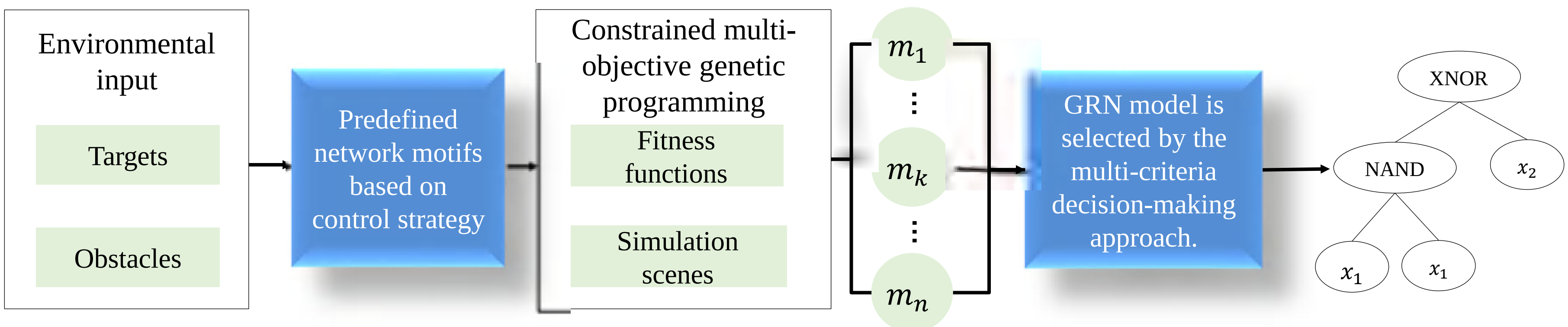

Swarm Coordination Mechanisms and Environmental Sensing Technologies Based on Stigmergy

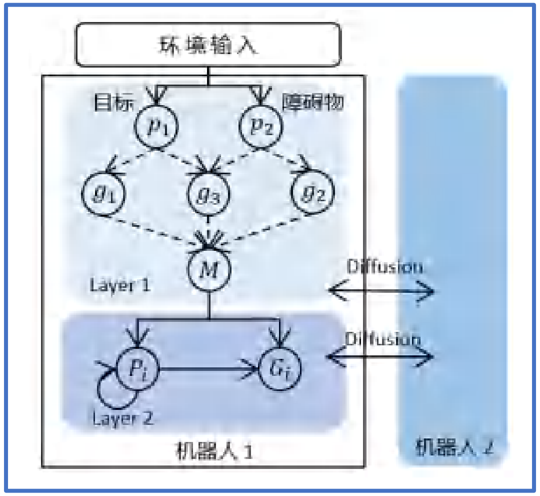

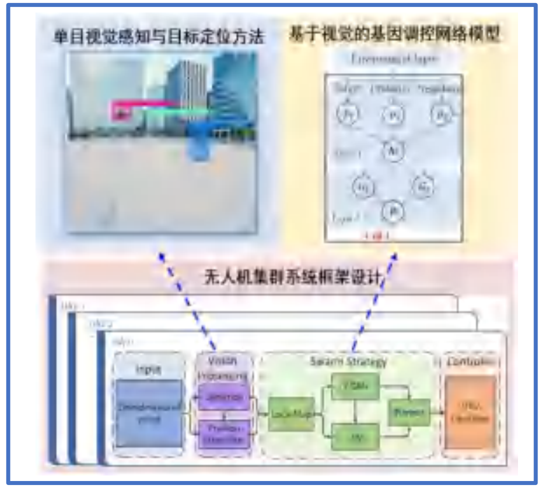

① Mapping of Swarm Behavior and Individual Behavior

② Communication Denied Environments

③ Challenges of Multiple Scenes and Multiple Perspectives

Design Automation of Swarm Behavior Coordination Strategies

Emergence of Swarm Behaviors without Communication

Ranging and Positioning of a UAV Swarm in Multiple Scenarios

Design Automation for Swarm Behavior Control

SHANTOU UNIVERSITY 汕頭大學

➢ Gene Regulatory Network Models

Amoeba movement

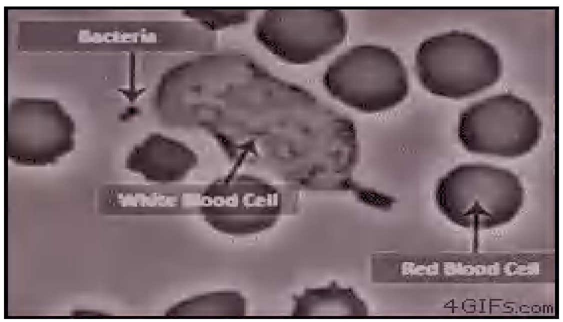

Leukocyte engulfs bacteria

No.	Gene regulatory Network model	Traditional control methods
1	The swarm pattern can adapt its shape according to the surrounding environment.	The swarm pattern should be fixed and known in advance.
2	This method does not require precise modeling of the swarm robot and is easy to deploy in practice.	This method requires precise modeling of the swarm system and is challenging to deploy in practice.
3	This method does not require the exact positions of the robots.	This method requires the exact positions of the robots.
4	This method can accomplish tasks in scenarios not only involving local communication, but also in communication denial, and even no-communication environments.	This method requires a fully connected communication network.

➢ Advantages of GRN models

➢ The GRN model can be efficiently integrated with traditional control algorithms[1][2]

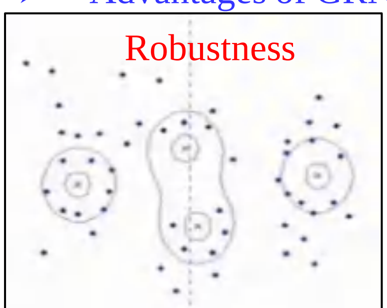

Fig.1. Unnecessary to locate robot exactly

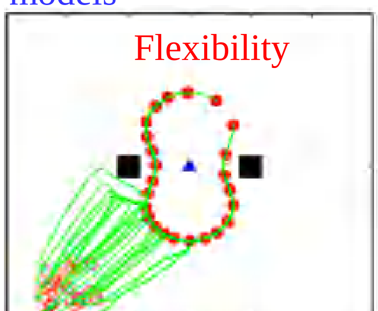

Fig2. Swarm pattern can be changed according to the environment.

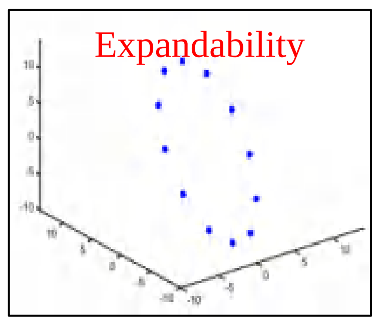

Fig. 3. No need communication networks

1. Zou A M, **Fan Z.** Distributed fixed-time attitude coordination control for multiple rigid spacecraft[J]. *International Journal of Robust and Nonlinear Control*, *30(1): 266-281,2020.*
2. Zou A M, **Fan Z.** Fixed-time attitude tracking control for rigid spacecraft without angular velocity measurements[J]. *IEEE Transactions on Industrial Electronics*, *67(8): 6795-6805, 2019.*

Design Automation for Swarm Behavior Control

汕頭大學 SHANTOU UNIVERSITY

We employ the same design automation framework to achieve the automated design of swarm behavior coordination strategies.

◆ The proposed method can automatically generate gene regulatory networks for swarm behaviors to form entrapping patterns to encircle escaping targets in dynamic environments..

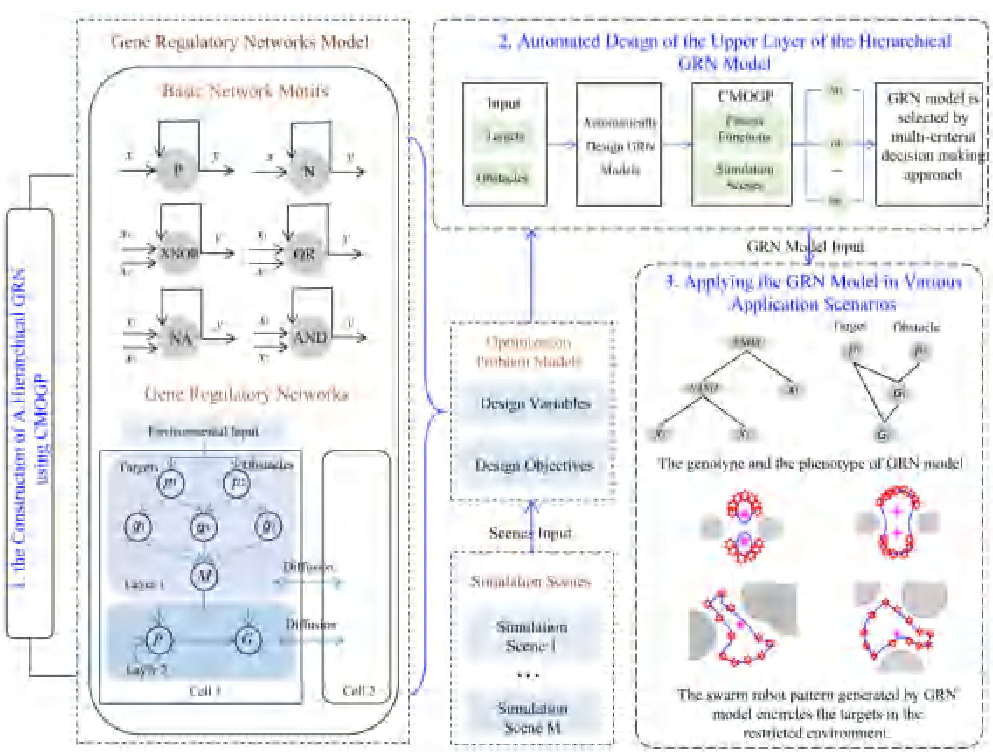

Fig.1. Diagram of the proposed design automation framework for generating entrapping patterns.

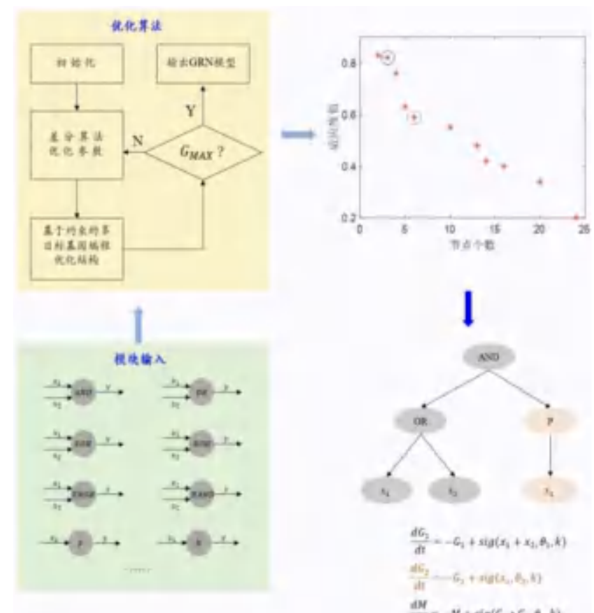

Fan Z, Wang Z, Li W, et al. **Automated pattern generation for swarm robots using constrained multi-objective genetic programming**[J]. ***Swarm and Evolutionary Computation***, 2023, 101337 (SCI 1区TOP期刊， IF = 10.0)

- The proposed GRN model can adapt the swarm's behavior to the environment, allowing a swarm of robots to entrap an escaping target. The initially scattered swarm organizes itself into an entrapping pattern over time.

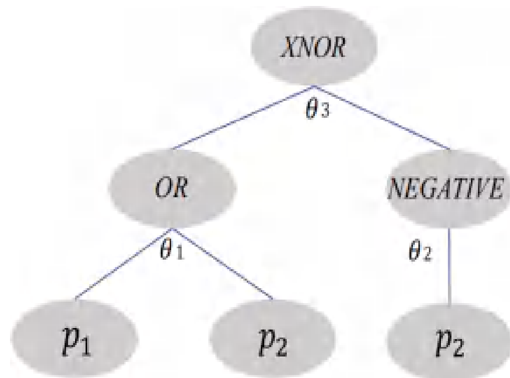

Fig. 1. Example of a GRN model

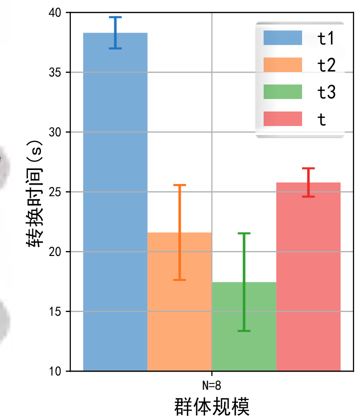

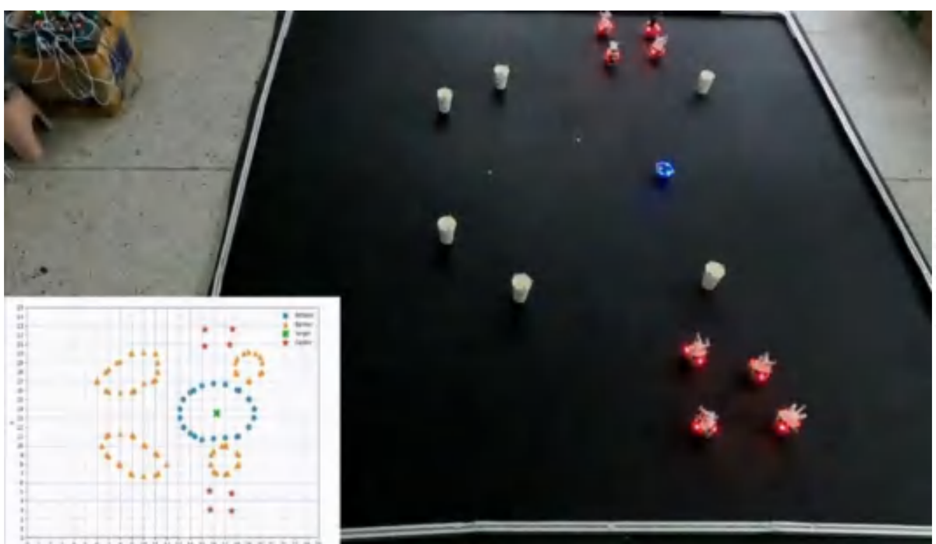

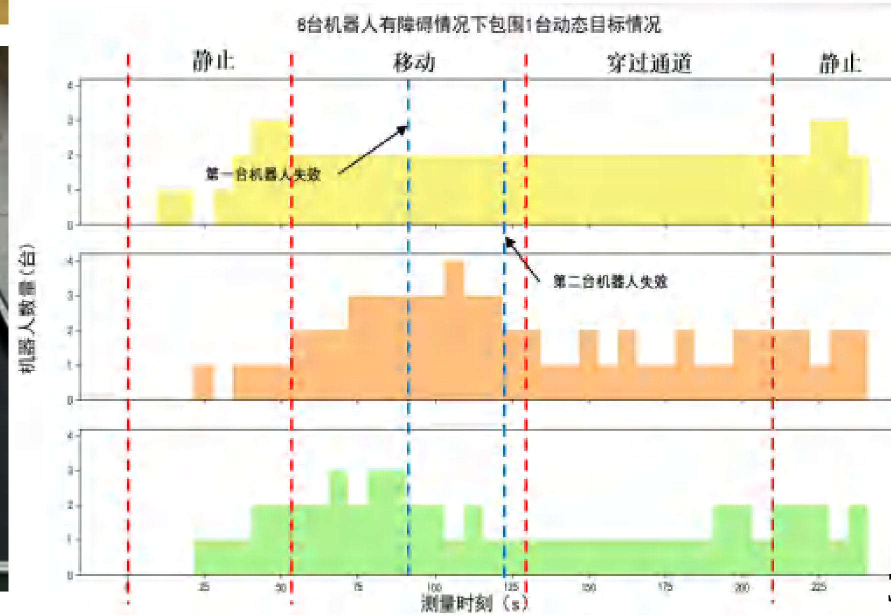

The entrapping pattern generated by our proposed method entraps two targets in an environment with obstacles

Swarm Control Without Communication

汕頭大學 SHANTOU UNIVERSITY

Emergence of UAV Swarm Behaviors in No-Communication Conditions

object detection and object position estimation

地图构建

object := [X; Y; Z; x; y; W; H; T; N]

分量计算

$$D = \alpha A^{\beta} \qquad X = \frac{2x \times D \times \sin\frac{FOV_h}{2}}{W}$$

$$Y = \sqrt{D^2 - X^2} \qquad Z = \frac{2y \times D \times \sin\frac{FOV_v}{2}}{H}$$

实验结果

在10米范围内测距误差均低于6%，以较低的硬件要求实现了全向视觉环境感知

a vision-based gene regulatory network

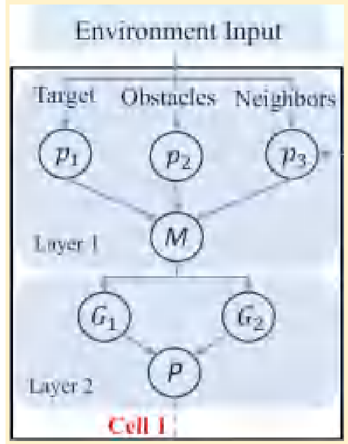

环境输入

$$\frac{dT_i}{dt} = \nabla^2 T_i + \gamma_i - T_i$$

$$\frac{dO_j}{dt} = \nabla^2 O_j + \beta_i - O_j$$

$$\frac{dN_m}{dt} = \nabla^2 N_m + \eta_m - N_m$$

控制输出

$$T, O, N = \sum_{i=1}^{n_t} T_i, \sum_{j=1}^{n_o} O_j, \sum_{m=1}^{n_n} N_m$$

$$\frac{dM}{dt} = -M + sig(1 - T^2) + sig(O^2) + sig(N^2)$$

$$sig(x) = \frac{1}{1 + e^{-k(x-\theta)}}$$

The architecture of the proposed VG-Swarm

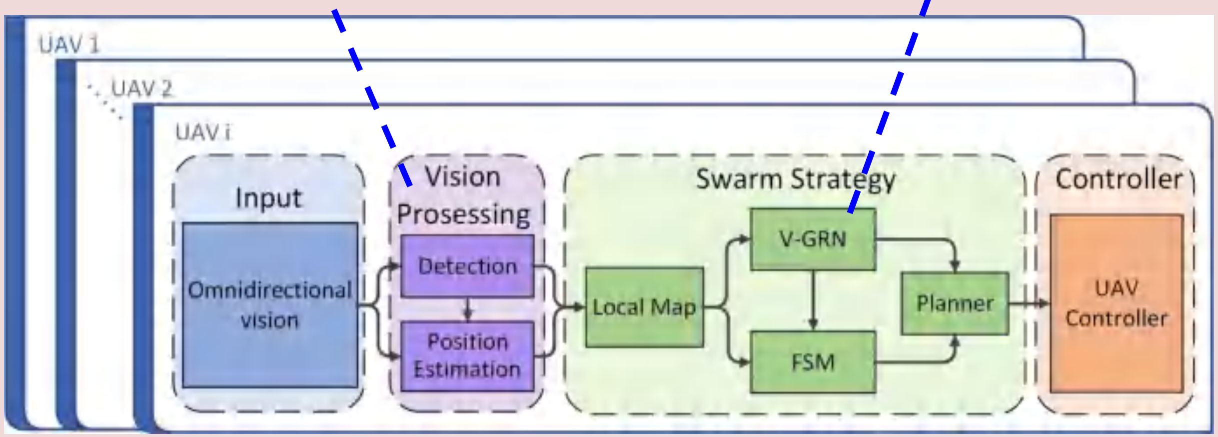

- The main contributions include a monocular visual perception and target localization method, and the design of a vision-based gene regulatory network model.
- The former is responsible for processing environmental input information, while the latter is responsible for regulating the motion of the UAV swarm using the processed information.

Swarm Control Without Communication

Entrapment Task

- The swarm of UAVs do not require direct communication among themselves. They rely solely on visual information for entrapping.
- Even in the presence of strong electromagnetic interference, the swarm can successfully entap the target using only visual information.

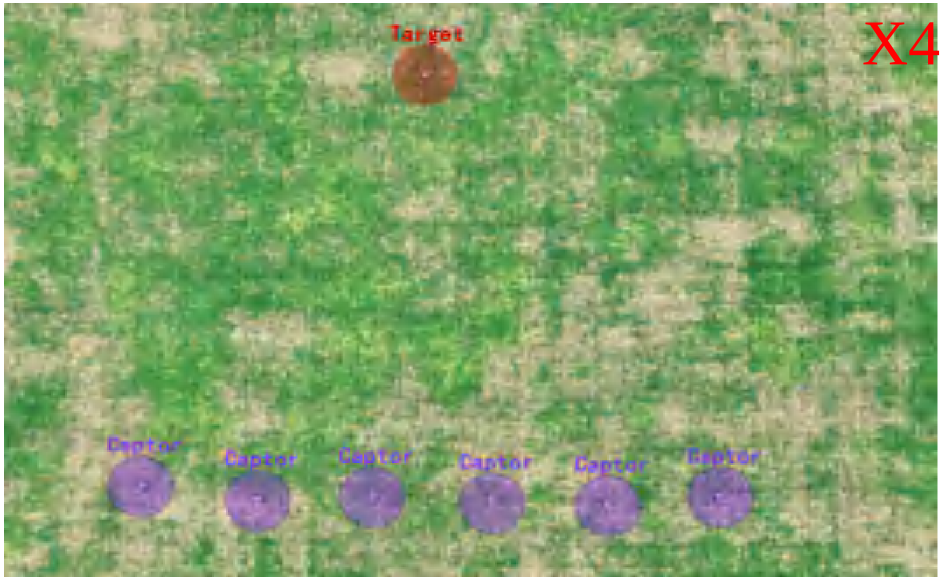

- Four drones swiftly move towards the target upon detection and achieve a stable entrapment of the dynamically moving target.
- Six drones entrap a moving target, and even when the target attempts to escape, the drones can continue to entrap it.

Allocation of Resources

- The drones can independently share resources within the swarm using visual information, without the need for communication. Even if the target escapes, the swarm can regroup and entrap it autonomously.

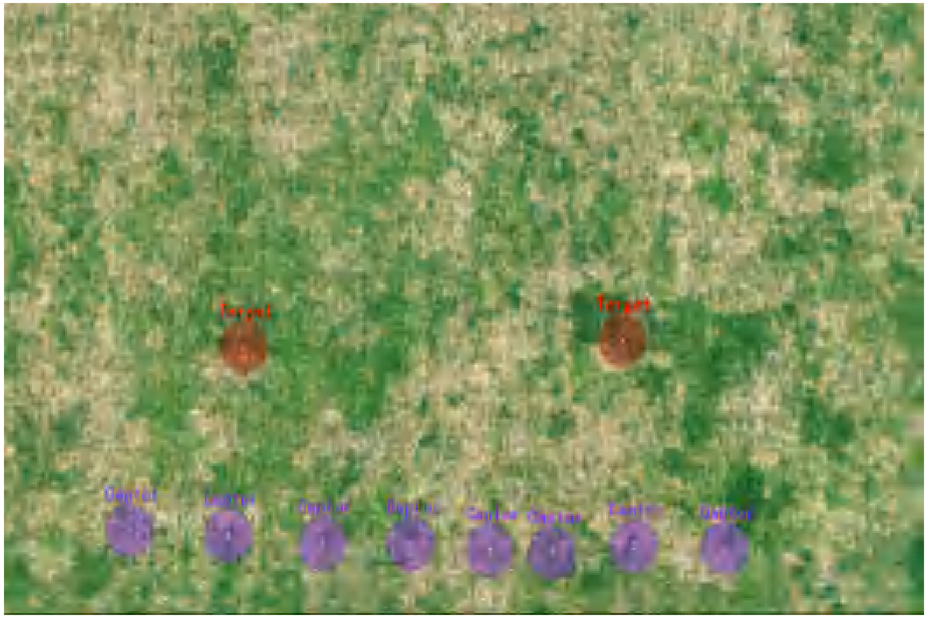

Ten drones autonomously coordinate to capture two targets, and even when the targets escape, the swarm can still autonomously allocate resources and complete the entrapment task.

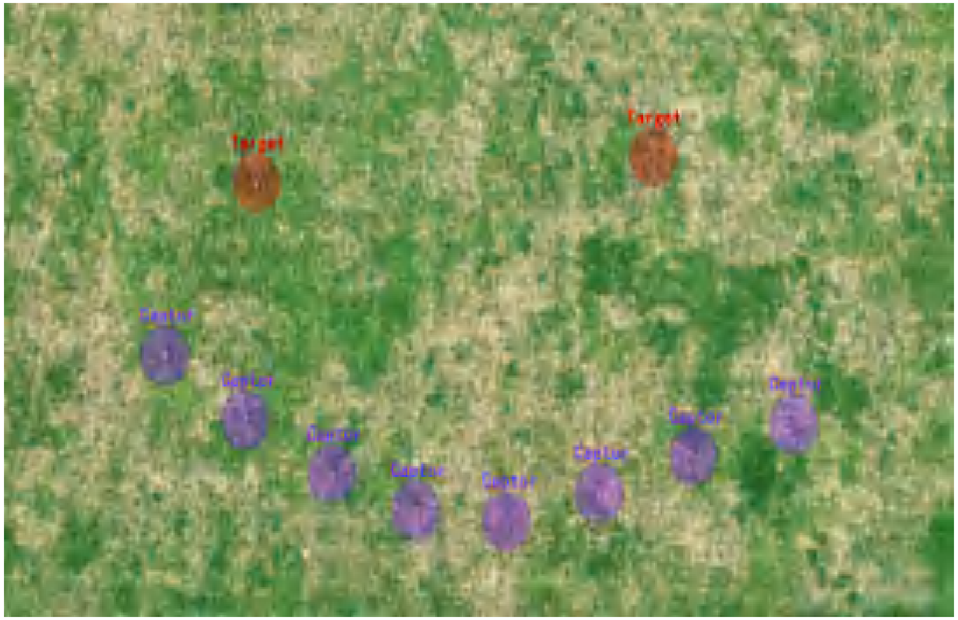

Ten drones autonomously coordinate to capture two targets. Even when some drones become disfunctional, the swarm can still manage to re-allocate the resounces and complete the entrapment task.

Swarm Control Without Communication

汕頭大學
SHANTOU UNIVERSITY

Target Search

- Drones do not require communication and rely solely on vision for environmental perception.
- The following video demonstrates drones using only vision for target search, tracking, and entrapment after their communication is disrupted in a communication-denied environment.

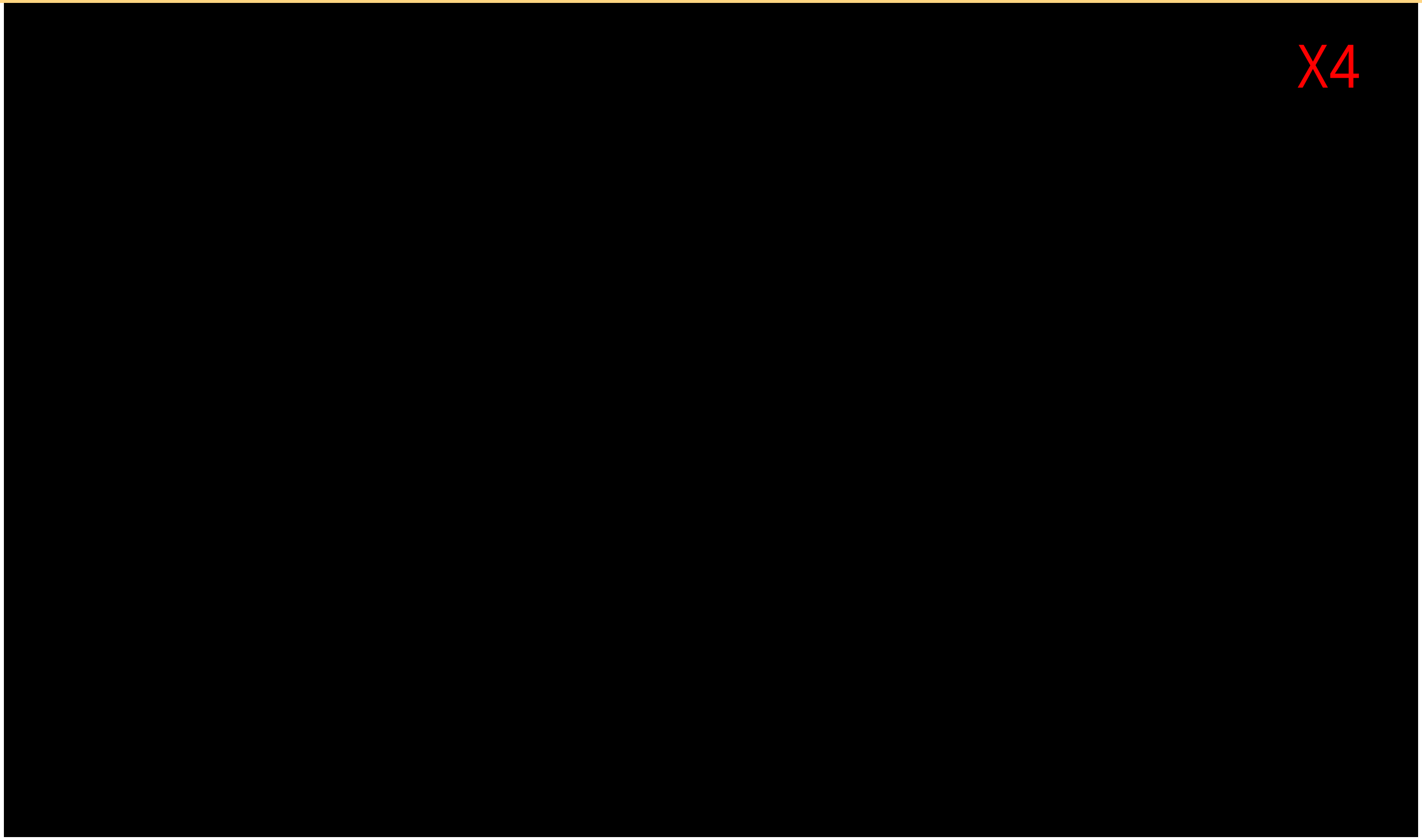

Improvement and Deployment of Target Detection Algorithm

SHANTOU UNIVERSITY 汕頭大學

We have proposed a real-time **tiny object detection algorithm** based on an improved YOLOv5 model

- We improved the Neck by deriving a prediction head from a higher-resolution feature map.
- Our method greatly reduces the model's parameters without compromising on average detection accuracy, achieving a detection speed that is twice as fast as YOLOv5s.

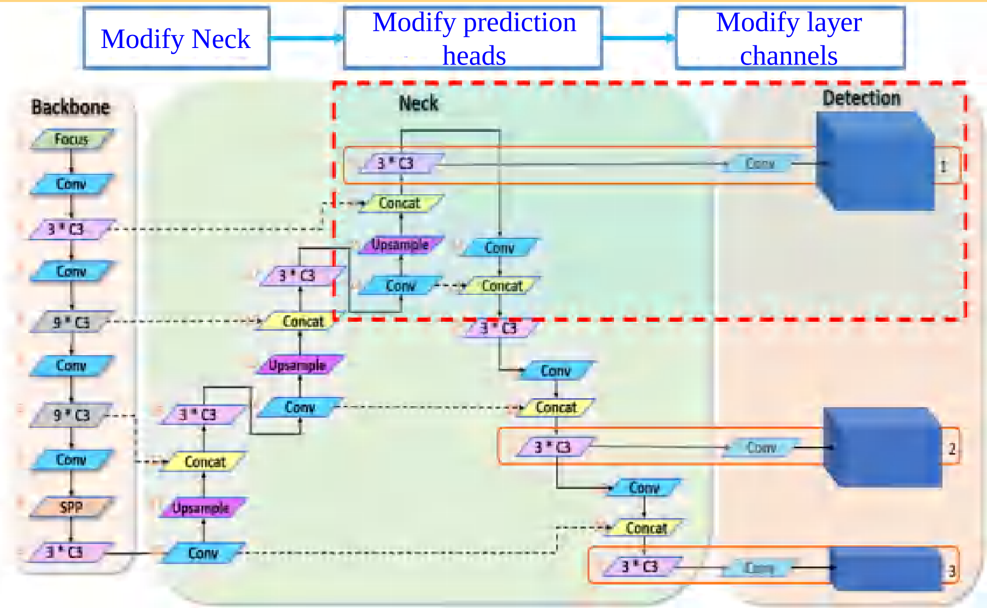

Fig. 1. Structure of small target detection model based on improved YOLOv5

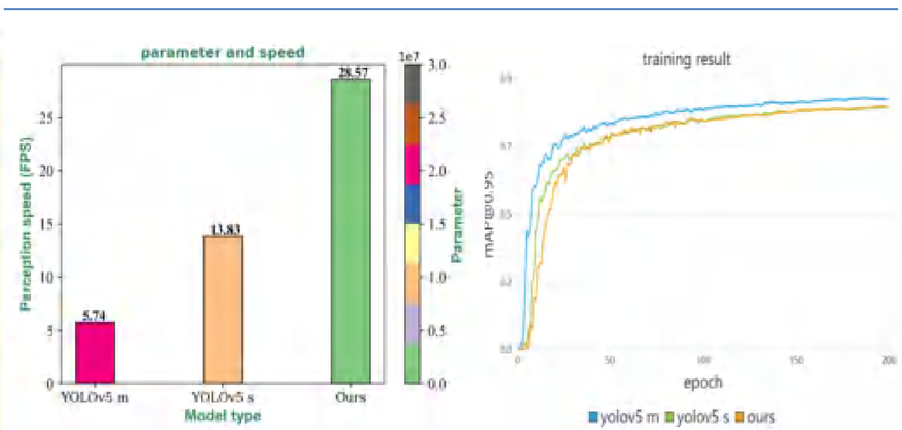

Fig 2. Experimental results of detection algorithm for small targets based on improved YOLOv5

- The proposed algorithm has only 17.4% of the parameters of the YOLOv5s model, and with Tensor RT acceleration, the system's omni-directional visual perception speed can reach 28 FPS.

Huanlin Li,Yuwei Cai, Junchao Hong, **Zhun Fan*,** et al. **VG-Swarm: A Vision-based Gene Regulation Network for UAVs Swarm Behavior Emergence.** *IEEE Robotics and Automation Letters, 2023, 1175 – 1182.*

Improvement and Deployment of Target Detection Algorithm

We propose a target localization method based on a monocular camera

- Our method fits the relationship between detection boxes and distance using multiple sets of observation points and depth information.
- It estimates the target's spatial position using the camera's Field of View and projection relationships.
- In real machine experiments, the ranging accuracy within 10 meters exceeds 93% (using UWB as the gold standard).

Huanlin Li,Yuwei Cai, Junchao Hong, **Zhun Fan*,** et al. **VG-Swarm: A Vision-based Gene Regulation Network for UAVs Swarm Behavior Emergence.** *IEEE Robotics and Automation Letters, 2023, 1175 – 1182.*

Summary

Using the same design automation framework, we have achieved automated design of morphologies (body), vision systems (eye), and coordination strategies (brain) for swarm robots, therefore advocating a novel method of integrated design of the 'body-eye-brain' of robotic systems.

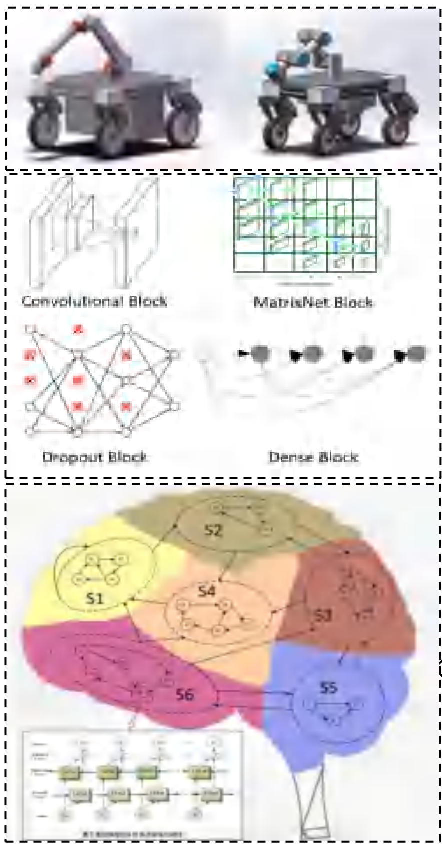

深度神经网络设计自动化

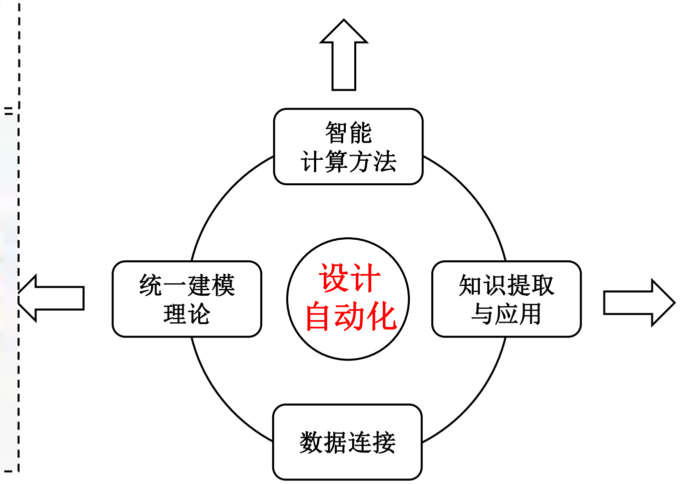

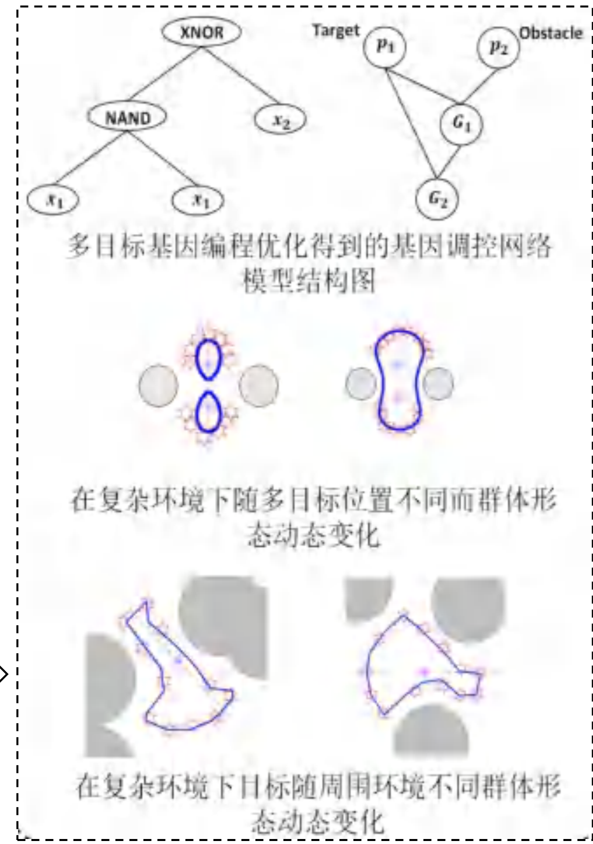

机器人'肢—眼—脑' 设计自动化

群体机器人自组织行为设计自动化

The Framewok of MODENA (MOdular DEsigN Automation)

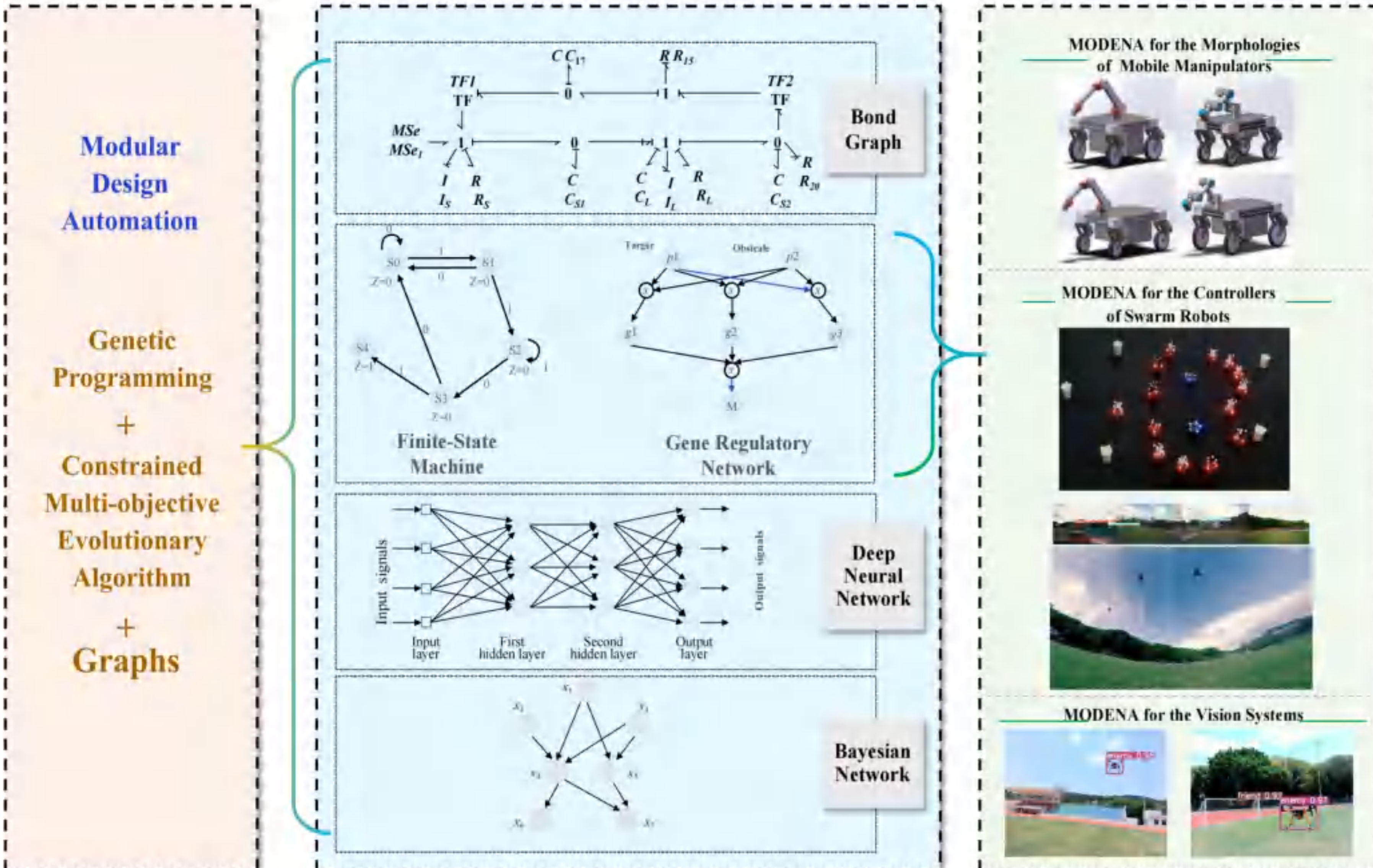

W. Li, Z. Wang, R. Mai, P. Ren, Q. Zhang, Y. Zhou, N. Xu, J. Zhuang, B. Xin, L. Gao, Z. Hao, **Z. Fan***. **Modular Design Automation of the Morphologies, Controllers, and Vision Systems for Intelligent Robots: A Survey**[J], ***Visual Intelligence***, 2023, 1(1), 3-30. (中国科技期刊卓越行动计划高起点新刊)

Thank you for your attention!

汕頭大學
SHANTOU UNIVERSITY

Collaborations Welcomed！

广东省进化智能与机器人国际合作基地

汕头大学人工智能与机器人实验室

主任：范 衡（教授、博导）

E-mail：zfan@stu.edu.cn， 电话：15218977996

地址：广东省汕头市大学路243号

实验室网页：http://imagelab.stu.edu.cn（欢迎扫码关注）

Multi-UAV Collision Avoidance via Deep Reinforcement Learning for Navigation

- The proposed method learns a strategy that can be directly transferred to different scenes, allowing for collision-free movement to target points.

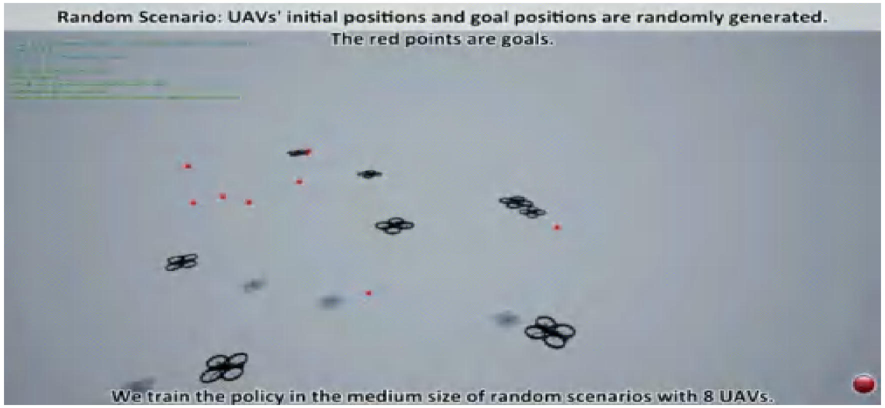

Video 1. Learn strategies of navigation and obstacle avoidance

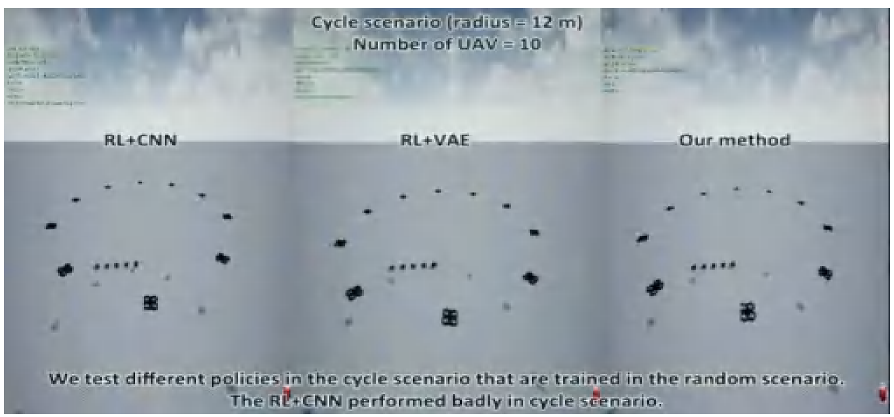

Video 2. The method proposed compared with other methods

Huang H, Zhu G, Zhu, **Fan Z***, Hao Z, et al. *Vision-based Distributed Multi-UAV Collision Avoidance via Deep Reinforcement Learning for Navigation*[C]. IEEE RSJ International Conference on Intelligent Robots and Systems (IROS). 2022, 1-8.

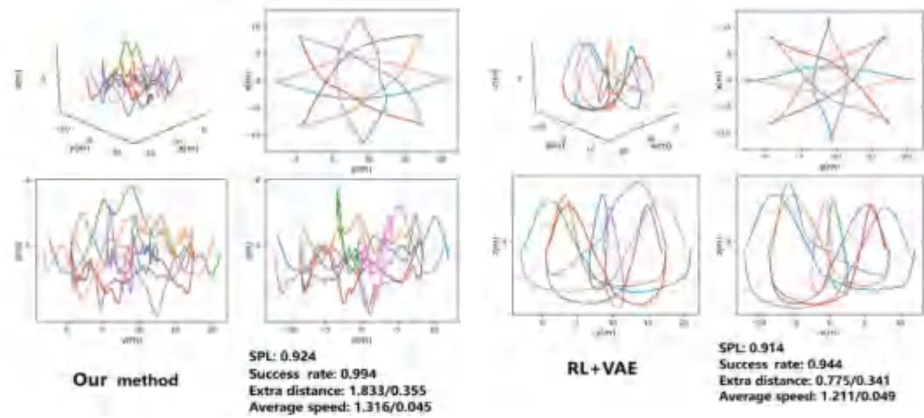

Fig. 1. Moving trajectories and navigation performance of 8 UAVs under different methods

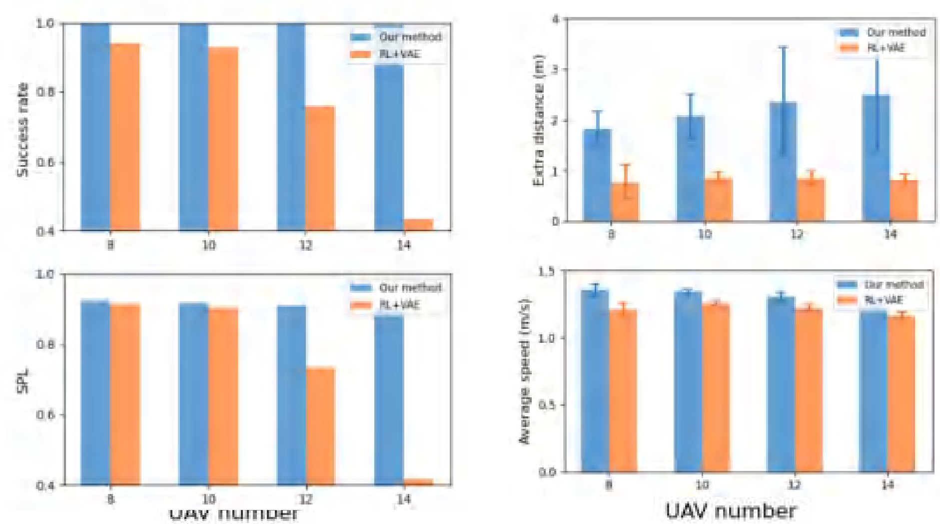

Fig. 2. The navigation performance of UAVs under different methods and different quantities

Pavement Crack Detection Based on a Lightweight Encoder-Decoder Network

An innovative hybrid attention module is proposed to focus on the crack region, thereby enhancing the network's feature expression capability.

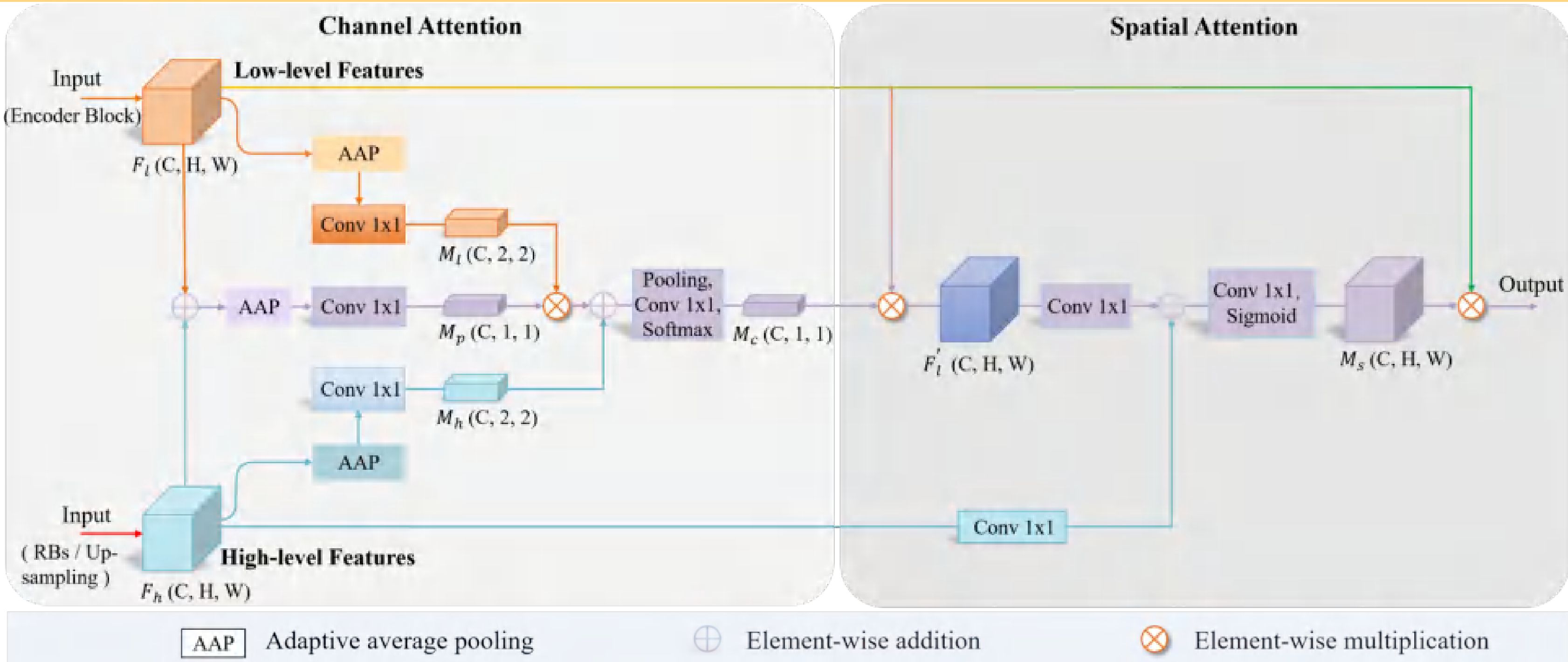

Schematic of the proposed hybrid attention block (HAB)

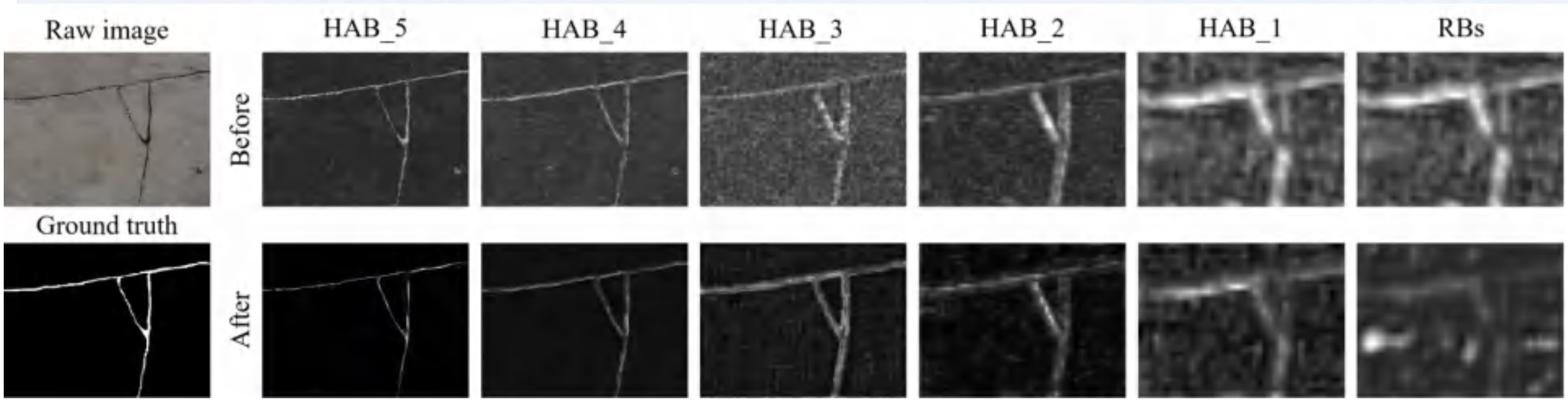

Visualization of the feature map

Pavement Crack Detection Based on a Lightweight Encoder-Decoder Network

汕頭大學 SHANTOU UNIVERSITY

An innovative hybrid attention module is proposed to focus on the crack region, thereby enhancing the network's feature expression capability.

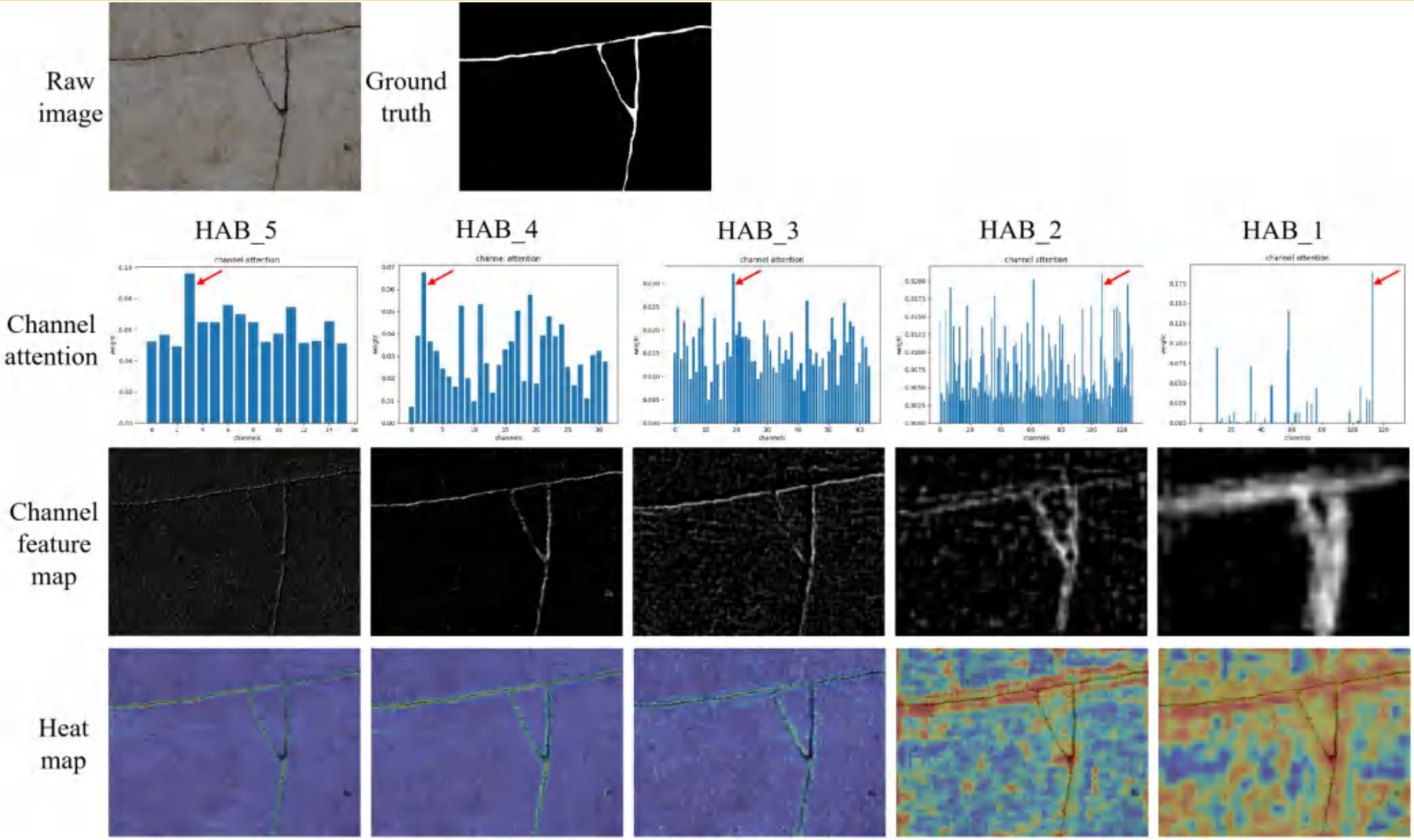

Fig1. Visualization of channel attention maps and spatial attention maps for each HAB

Pavement Crack Detection Based on a Lightweight Encoder-Decoder Network

汕頭大學 SHANTOU UNIVERSITY

For tiny cracks with complex topologies, the proposed model using the hybrid attention module performs better than models with other attention mechanisms.

Table 1. Results of comparison with different attention mechanisms on CamCrack789 and CFD

Models	CamCrack789			CFD		
	Pr	*Re*	*F1*	*Pr*	*Re*	*F1*
SE	0.9139	0.9658	0.9366	0.9374	0.9359	0.9342
CBAM	0.9180	0.9621	0.9367	0.9429	0.9231	0.9303
ECA	0.9223	0.9640	0.9405	0.9269	0.9208	0.9161
DA	0.8835	**0.9784**	0.9258	0.9187	0.9107	0.9103
HAB	**0.9483**	0.9504	$\boxed{\mathbf{0.9494}}$	**0.9629**	**0.9520**	$\boxed{\mathbf{0.9574}}$

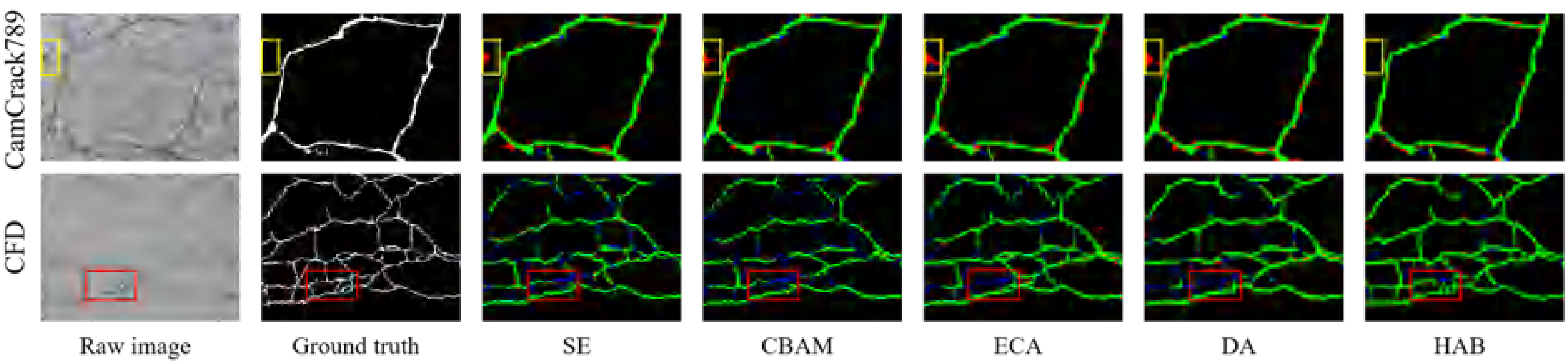

Fig1. Visualization results of methods of different attention modules

Pavement Crack Detection Based on a Lightweight Encoder-Decoder Network

汕頭大學 SHANTOU UNIVERSITY

Comparison with Existing Methods

TABLE 2 Experimental results on the CamCrack789 dataset.

Methods	Precision (*Pr*)	Recall (*Re*)	F1 score (*F1*)	Floating-point operations per second (FLOPs; G)	Time/image (s)
FCN [CVPR 2015]	0.9445	0.9440	0.9443	290.46	0.094
U-Net [MICCAI 2015]	0.9349	0.9401	0.9375	375.24	0.111
Attention U-Net [MIDL 2018]	0.9470	0.9495	0.9482	624.72	0.199
DC_Zou [TIP 2018]	0.9660	0.8455	0.9017	1283.64	0.361
DC_Liu [Neurocomputing 2019]	**0.9669**	0.8146	0.8843	188.56	0.058
DMA-Net [TITS 2022]	0.9377	0.9463	0.9420	212.12	0.068
AttentionCrackNet [CACAIE 2022]	0.9386	0.9450	0.9418	329.02	0.104
RHACrackNet	0.9483	**0.9504**	**0.9494**	21.60	0.033
RHACrackNet*	0.9494	0.9465	0.9480	**9.68**	**0.032**

TABLE 3 Experimental results on Crack500.

Methods	*Pr*	*Re*	*F1*	FLOPs (G)	Time/image (s)
FCN [CVPR 2015]	0.8067	0.8385	0.8223	61.96	0.023
U-Net [MICCAI 2015]	0.7984	0.8464	0.8203	80.06	0.025
Attention U-Net [MIDL 2018]	0.8129	0.8345	0.8235	133.28	0.045
DC_Zou [TIP 2018]	0.8058	0.7999	0.8028	273.84	0.082
DC_Liu [Neurocomputing 2019]	**0.8542**	0.7478	0.7975	40.22	0.015
DMA-Net [TITS 2022]	0.7426	**0.9183**	0.8204	45.23	0.018
AttentionCrackNet [CACAIE 2022]	0.7794	0.8570	0.8006	70.2	0.024
RHACrackNet	0.8061	0.8542	**0.8295**	4.60	**0.011**
RHACrackNet*	0.8173	0.8404	0.8287	**2.06**	**0.011**

Comparison with Existing Methods

TABLE 4 Experimental results on CFD.

Methods	*Pr*	*Re*	*F1*	FLOPs (G)	Time/image (s)
FCN [CVPR 2015]	0.8118	0.8510	0.8309	145.22	0.064
U-Net [MICCAI 2015]	0.8463	0.8809	0.8633	187.62	0.068
Attention U-Net [MIDL 2018]	0.9253	0.8844	0.9044	312.36	0.117
DC_Zou [TIP 2018]	0.9674	0.8088	0.8810	641.82	0.200
DC_Liu [Neurocomputing 2019]	**0.9890**	0.6065	0.7519	94.28	0.047
DMA-Net [TITS 2022]	0.9171	0.9453	0.9310	106.06	0.053
AttentionCrackNet [CACAIE 2022]	0.9430	0.9408	0.9399	164.52	0.066
RHACrackNet	0.9629	**0.9520**	**0.9574**	10.80	**0.030**
RHACrackNet*	0.9595	0.9359	0.9476	**4.84**	**0.030**

TABLE 5 Results of compared methods test on DeepCrack237 dataset.

Methods	*Pr*	*Re*	*F1*	FLOPs (G)	Time/image (s)
FCN [CVPR 2015]	0.9049	0.8886	0.8967	197.50	0.152
U-Net [MICCAI 2015]	0.9206	0.9130	0.9168	255.16	0.178
Attention U-Net [MIDL' 2018]	0.9284	0.9121	0.9202	424.80	0.317
DC_Zou [TIP 2018]	0.9481	0.8041	0.8702	872.88	0.585
DC_Liu [Neurocomputing 2019]	**0.9790**	0.7131	0.8252	128.22	0.107
DMA-Net [TITS 2022]	0.9421	0.9072	0.9241	144.24	0.127
AttentionCrackNet [CACAIE 2022]	0.9079	0.9052	0.8899	223.74	0.164
RHACrackNet	0.9364	**0.9141**	**0.9251**	14.68	**0.083**
RHACrackNet*	0.9312	0.9139	0.9226	**6.58**	**0.080**

● Visualization results

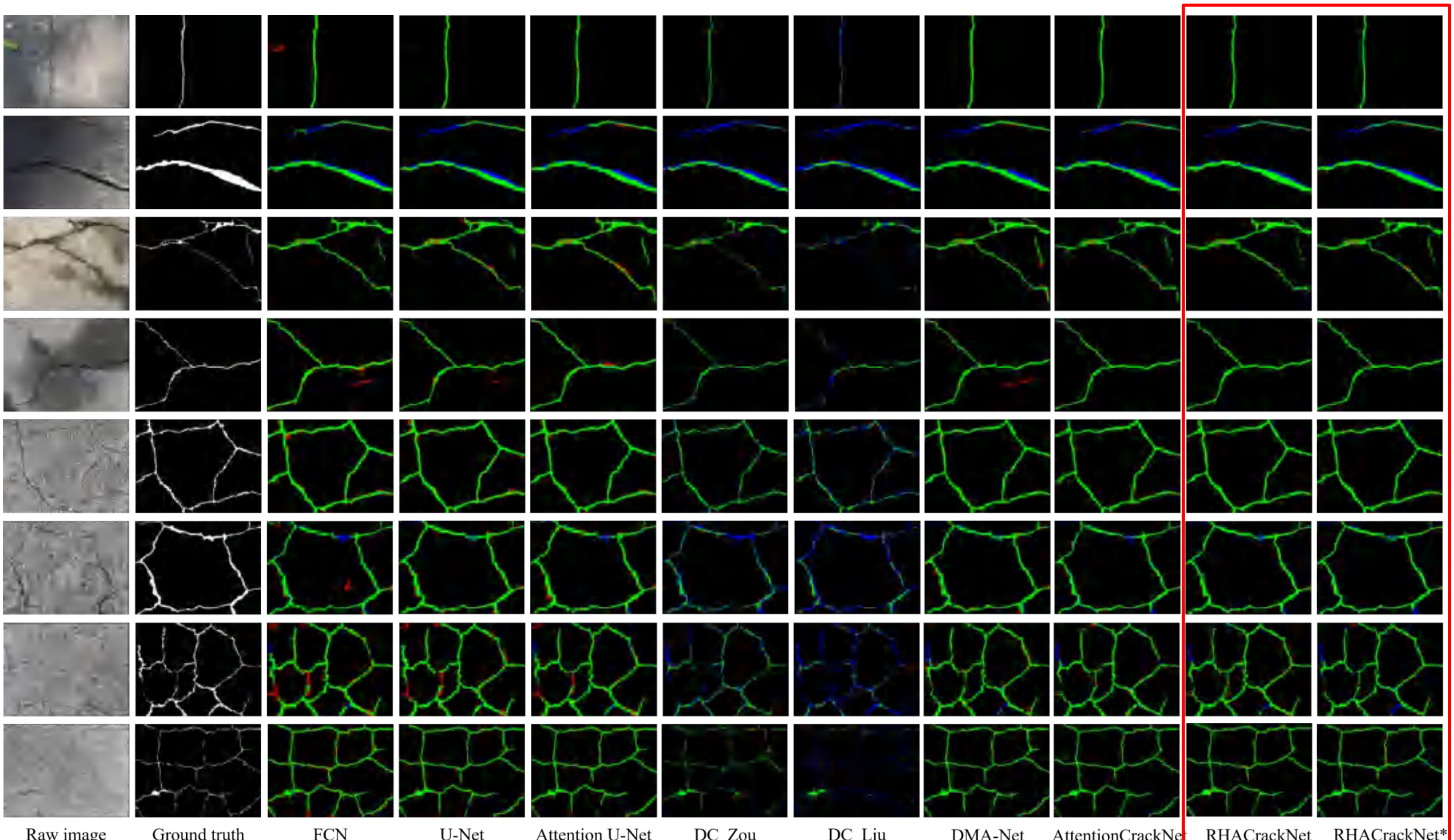

Fig. Visualization results of different models from the CamCrack789 dataset. The green, red, and blue pixels in the images represent true positives, false positives, and false negatives, respectively.

Pavement Crack Detection Based on a Lightweight Encoder-Decoder Network

SHANTOU UNIVERSITY

● Visualization results

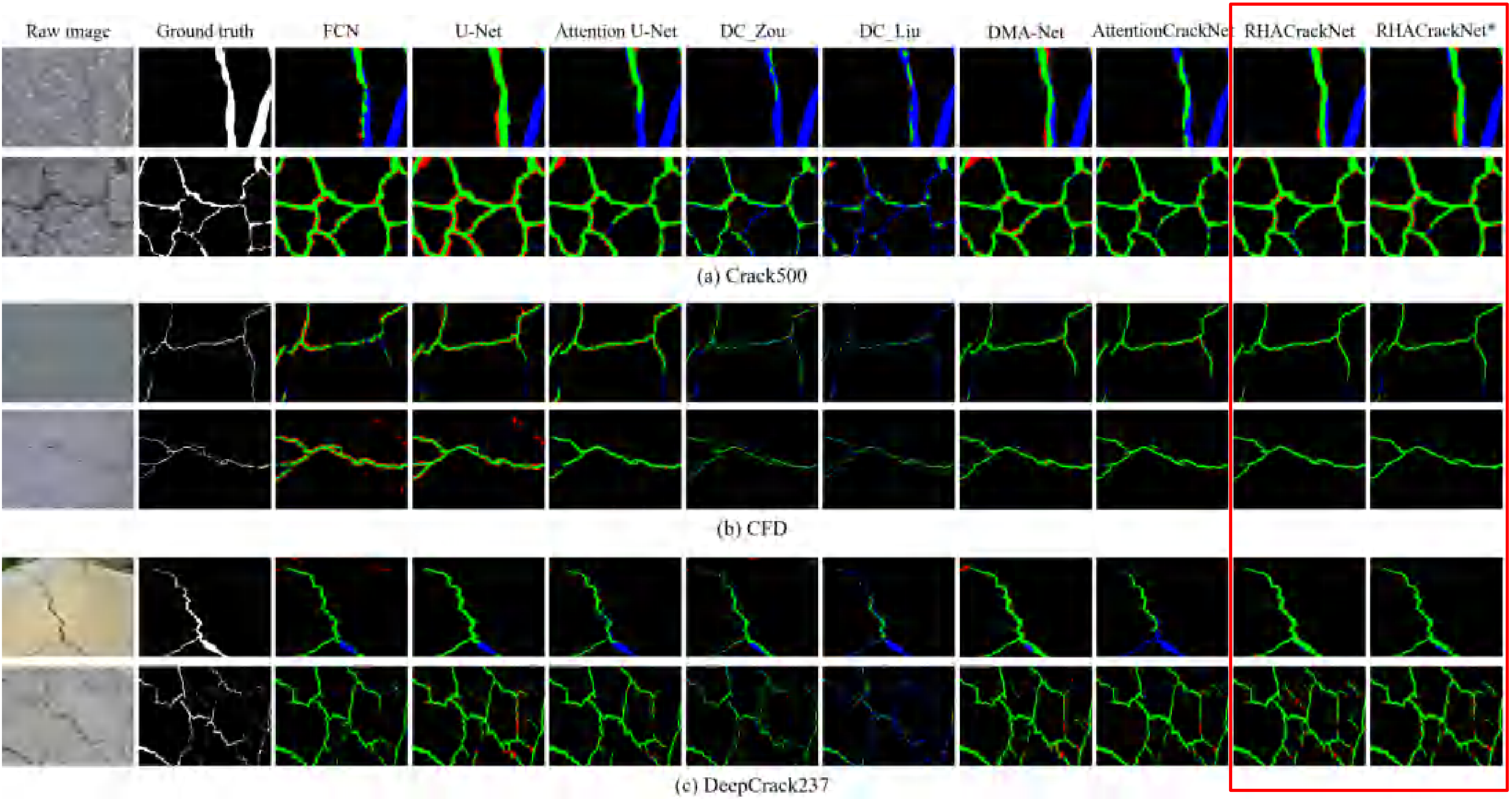

Fig. Visualization results of different models from Crack500, CFD, and DeepCrack237.

Background

汕頭大學 SHANTOU UNIVERSITY

AutoGPT

AutoGPT autonomously breaks down a set goal into smaller tasks and completes them without human intervention, ensuring efficient and independent achievement of objectives.

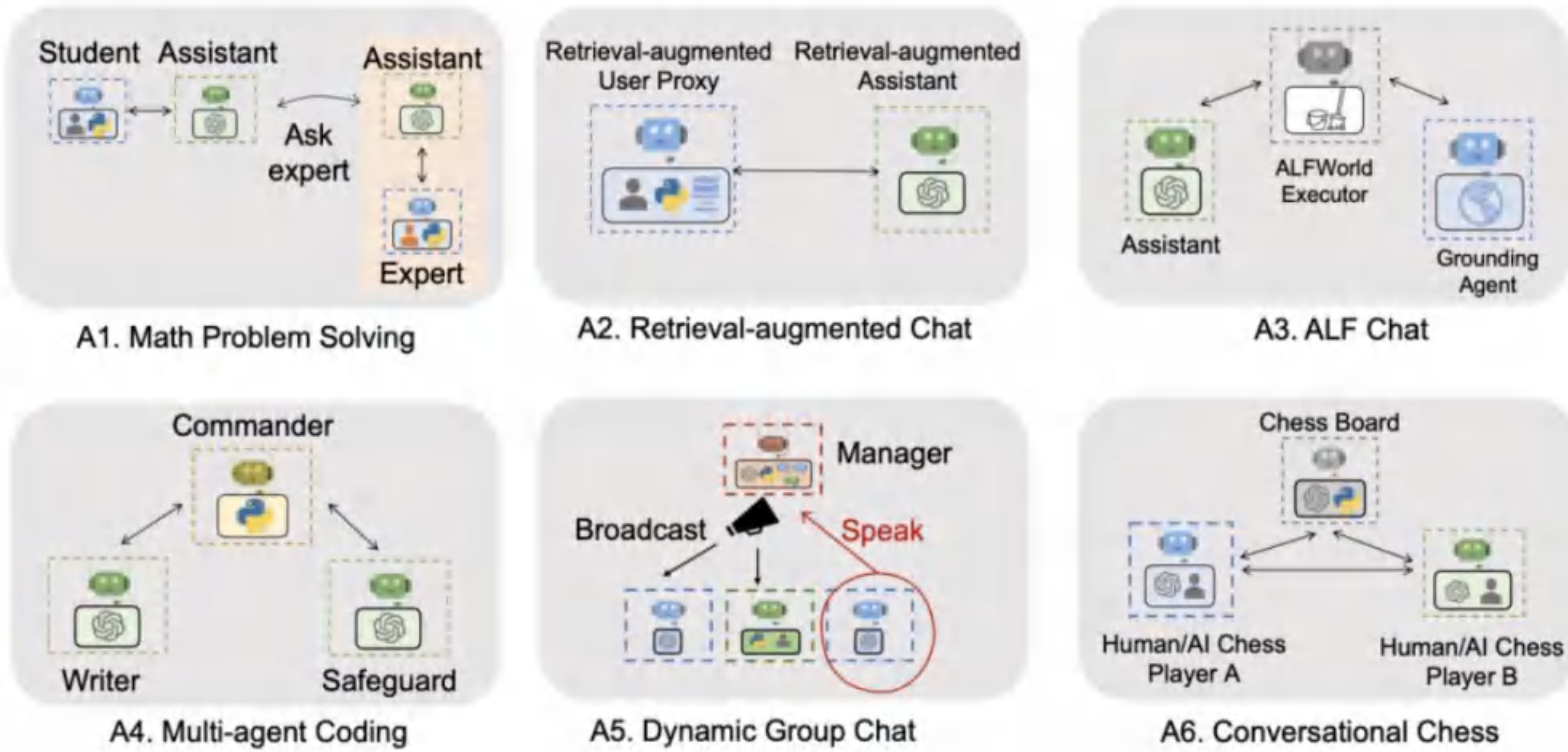

AutoGPT can handle tasks like solving mathematical problems, performing enhanced retrieval chat, ALF chat, multi-agent coding, dynamic group chatting, playing chess, and more.